C67

Release-independent short-term depression of synaptic transmission: does it exist?

K. Volynski and D.M. Kullmann

Institute of Neurology, UCL, London, UK

Synapses almost universally show a dependence of release probability on the recent history of activity: they facilitate or depress, and a number of mechanisms have been suggested to mediate this phenomenon, most prominent of which are delayed clearance of calcium ions from the presynaptic terminal and depletion of readily releasable vesicles. However, an intriguing phenomenon is revealed by several studies (e.g. [1]) that have looked at individual synapses with very short intervals between two presynaptic stimuli: the probability of observing a quantal release event is profoundly decreased on the second trial, not only when the first trial resulted in a release event, but also when the first trial resulted in a failure of release.

The typical way that 'release-independent depression' is demonstrated is by repeatedly probing the synapse with paired stimuli, and sorting the results into several outcomes. Let us denote the probability of observing two failures as P(0,0), of observing a failure followed by a success as P(0,1), a success followed by a failure as P(1,0), and two successes as P(1,1). The reported result is that the success rate for the second response, if the first trial resulted in a failure, is lower than the overall success rate for the first trial: $P(0,1)/(P(0,0)+P(0,1)) < P(1,0)+P(1,1)$.

Several mechanisms have been proposed to underlie this 'release-independent depression', including failure of action potential invasion and calcium channel inactivation, although none of these has been conclusively demonstrated. We argue here that release-independent depression may actually be an illusion, resulting from an unrealistic assumption that the initial state of the synapse is constant across all the trials.

Indeed, it is commonly accepted that at single synapse probability of neurotransmitter release in response to an action potential is determined by the number of release ready vesicles (RRV), n, and by the average probability of release for a single RRV, Pves. Accumulating data suggest that instantaneous probability of release at a given synapse can fluctuate from trial to trial due to fluctuations in both n and Pves [2,3]. Taking into account these observations we used Monte-Carlo simulations to demonstrate that stochastic fluctuations in instantaneous probability of release can give rise to apparent release-independent depression as a result of sampling bias. The time course of the relationship between this apparent depression and inter-stimulus interval provides a window on the kinetics of state transitions of the release apparatus.

Dobrunz LE, Huang EP & Stevens CF (1997). Proc Natl Acad Sci U S A 94, 14843-14847.

Hanse E & Gustafsson B (2001). J Physiol 531, 481-493.

Sudhof TC (2004). Annu Rev Neurosci 27, 509-547.

Where applicable, the authors confirm that the experiments described here conform with the Physiological Society ethical requirements.

C68

Unitary connections and heterogeneity of presynaptic calcium channels of hippocampal oriens/alveus interneurons *in vitro*

D. Elfant[1], B. Pal[1], N. Emptage[2] and M. Capogna[1]

[1]MRC Anatomical Neuropharmacology Unit, Oxford University, Oxford, UK and [2]Department of Pharmacology, Oxford University, Oxford, UK

Distinct populations of GABAergic interneurons located in the stratum oriens (SO) of the hippocampus are characterised by a horizontal somatodendritic architecture and axon that projects into the stratum radiatum (SR) or lacunosum moleculare (SLM). Such interneurons may act as feedback regulators of CA1 pyramidal cell activity receiving excitatory postsynaptic potentials (EPSPs) from pyramidal axon collateral branches in SO and in turn innervating the distal dendrites of pyramidal cells in the SLM and evoking inhibitory postsynaptic potentials (IPSPs) (1). Anatomical data, however, suggests that these interneurons have synaptic targets not only on the distal dendrites of pyramidal cells but also on GABAergic elements (2). The properties of these interneuron-interneuron synapses are not known. Therefore, electrophysiological recordings were performed on acute slices and slice cultures from juvenile rats. Recorded neurons were filled with biocytin and analysed post-hoc. Minimal stimulation of SO elicited unitary inhibitory postsynaptic currents (uIPSCs) in interneurons located in SR and SLM. The uIPSCs recorded with a K-gluconate-based patch solution at -50mV had an amplitude of 20.3 ± 5pA, rise time 2.1 ± 0.3ms, decay 21.8 ± 2.9ms and jitter 1.1 ± 0.3ms (average ± SEM, n=12). Interestingly, uIPSCs were sensitive to either the N-type calcium channel antagonist conotoxin MVIIA (1μM, n=4), or the P/Q-type calcium channel antagonist agatoxin IVA (200nM, n=4) or both (n=4). Paired recordings between interneurons in SO and SR or SLM showed uIPSCs with similar kinetic properties, namely amplitude of 15.6 ± 1.3pA, rise time 2.3 ± 0.5ms, decay 30.7 ± 8.2ms and jitter 1.3 ± 0.3ms (average ± SEM, n=11). Likewise, these uIPSCs were sensitive to conotoxin MVIIA (1μM, n=2) or agatoxin IVA (200nM, n=1) or both (n=3). The uIPSCs had a stable control amplitude for at least 1h and were abolished by 1.2μM gabazine (n=5). We are currently investigating whether there is a correlation between the postsynaptic interneuron type and the physiological and pharmacological properties of the synapse. Calcium transients were imaged at a single SLM varicosity of the axon of interneurons with the soma in SO (n=2) in order to study the action of calcium channel antagonists. We demonstrate the existence and properties of unitary connections between interneurons in SO and their interneuron target(s) in the SR and SLM, providing a direct link between CA1 feedback and feed-forward inhibitory interneurons. Different calcium channels can be functional within an individual connection enriching the view that release at inhibitory synapses in the hippocampus is initiated by a unique class of calcium channel.

Maccaferri G (2005). *J Physiol* **562**, 73-80.

Katona *et al.* (1999). *Neuroscience* **88**, 37-57.

Funded by the MRC UK.

Where applicable, the authors confirm that the experiments described here conform with the Physiological Society ethical requirements.

C70

Contrasting voltage-dependent properties of $GABA_A$ receptors mediating phasic and tonic conductances in the hippocampal CA1 pyramidal cells

I. Pavlov[1], A. Semyanov[2], D.M. Kullmann[1] and M.C. Walker[1]

[1]Department of Clinical and Experimental Epilepsy, Institute of Neurology, London, UK and [2]Neuronal Circuit Mechanisms Research Group, The Institute of Physical and Chemical Research (RIKEN) Brain Science Insitute, Wako-shi, Japan

$GABA_A$ receptor-mediated signalling in the brain can be divided into phasic inhibition, due to transient activation of synaptic receptors, and tonic inhibition, mediated by persistent activation of extrasynaptic receptors. These two forms of signalling have been proposed to have different roles in information processing (Farrant & Nusser, 2005). We, therefore, asked if these two forms of signalling show distinct voltage dependencies.

To address this question, we made whole-cell voltage clamp recordings from CA1 pyramidal cells in hippocampal slices from 3-4 week old rats. All experiments were carried out at 32°C. We isolated the $GABA_A$ receptor-mediated responses by applying ionotropic glutamate receptor and $GABA_B$ receptor antagonists. We measured the holding current during voltage ramps (-70 mV to +40 mV) before and after the application of the $GABA_A$ receptor antagonist picrotoxin (100 μM). We were thus able to determine the voltage dependence of the tonic current.

We found that, in contrast to synaptic currents, the tonic current demonstrates significant outward rectification. In addition, the tail but not peak of evoked IPSCs showed similar rectification, consistent with GABA spillover from the synaptic cleft onto extrasynaptic receptors. This rectification could be due to receptor properties or reversal of GABA transporters during depolarisation, leading to GABA accumulation. We therefore repeated the voltage ramp experiments in the presence of GAT-1 and/or GAT-2/3 blockers, SKF-89976A (30 μM) and SNAP-5114 (50 μM), respectively. Block of GABA uptake decreased, but did not abolish, the outward rectification. Rectification index decreased from 4.32±0.65 (control condition, n=11) to 2.85±0.29 (SKF-89976A, n=6, $p>0.05$) and 1.64±0.19 (SKF-89976A+SNAP-5114, n=3, $p<0.05$). This result is consistent with a component of the outward rectification being due to reversal of GABA uptake. Alternatively, elevated levels of GABA recruit an additional pool of less rectifying receptors that are otherwise not active under baseline conditions. Perfusing slices with GABA (30-20 μM) in the absence of GAT-1 and GAT-2/3 blockers yielded results similar to those with GABA transporters blocked (rectification index 2.33±0.15, $p<0.02$ as compared to control, n=9), arguing for the latter possibility.

Tonic conductances in CA1 pyramidal cells thus demonstrate marked outward rectification, which is due to receptor properties rather than local GABA accumulation with depolarisation. This outward rectification is likely to act as a homeostatic mechanism increasing tonic inhibition when neurons are depolarised.

Farrant & Nusser (2005). Nat Rev Neurosci 6, 215-229.

Where applicable, the authors confirm that the experiments described here conform with the Physiological Society ethical requirements.

C107

Short-term depression amplifies gain modulation by tonic inhibition in cerebellar granule cells

V. Steuber, J. Rothman, L. Cathala and R.A. Silver

Physiology, UCL, London, UK

Multiplicative gain modulations change the slope of the input-output relationship of neurons and alter their sensitivity to changes in excitatory inputs. They are observed frequently in vivo and are thought to play an important role for the processing of information in the brain [1]. A common feature of conditions where multiplicative modulation takes place is the presence of noise, either as background or in the driving inputs themselves [2-4]. As the amount of noise depends on the amplitude of synaptic inputs, synaptic plasticity is expected to affect the extent of gain modulation. In the cerebellum, synapses between mossy fibres (MFs) and granule cells (GCs) undergo short-term depression (STD) [5]. We used computer simulations and electrophysiological recordings to study the effect of STD on gain modulation by tonic inhibition in GCs. We injected depressing and non-depressing conductance trains into GCs in cerebellar slices and found that short-term depression (STD) of synaptic inputs resulted in a large enhancement of gain modulation by a tonic inhibitory conductance. STD has two effects: it reduces the amount of noise in the inputs, and it introduces a non-linear relationship between input rate and mean input conductance. Using a simple STD model, we could show that the effect of the non-linearity dominated the noise effect for all levels of STD. Our results suggest that the presence of STD at the MF-GC cell synapse could optimise gain modulation at the cerebellar input stage.

Salinas E & Thier P (2000). Neuron 27, 15-21.

Doiron B et al. (2001). Neural Comput 13, 227-248.

Chance FS, Abbott LF & Reyes AD (2002). Neuron 35, 773-782.

Mitchell SJ & Silver RA (2003). Neuron 38, 433-445.

Saviane C & Silver RA (2006). Nature 439, 983-987.

Supported by the MRC, the Wellcome Trust and the EC.

Where applicable, the authors confirm that the experiments described here conform with the Physiological Society ethical requirements.

C108

Functional synaptic connections between mouse cerebellar Purkinje cells

A.J. Watt, P.J. Sjöström, M. Mori, L. Ramakrishnan and M. Häusser

Wolfson Institute for Biomedical Research and Department of Physiology, University College London, London, UK

Cajal suggested a century ago that Purkinje cell (PC) collaterals make synaptic contacts with other Purkinje cells (1). However, direct demonstration of a functional connection between Purkinje cells has been lacking. We have used two transgenic mouse lines that express GFP in PCs to facilitate the anatomical and electrophysiological study of these connections. Sagittal slices (200 – 300 μm) were prepared from P4–P15 mouse cerebellar vermis and slices were maintained at 32-34°C. Two-photon laser scanning microscopy was used to visualize putative presynaptic PCs expressing GFP, and to follow their axon collaterals in order to target putative postsynaptic PCs. Simultaneous triple or quadruple somatic recordings were made from putative pre- and postsynaptic neurons in current clamp (I-clamp, K^+-based internal solution) or voltage clamp (V-clamp; Cs^+-based internal solution). Since the Cl^- reversal potential is known to hyperpolarize over the developmental period studied here (2), symmetrical Cl^- internal solution was chosen. Neurons were hyperpolarized to ~-65 mV to prevent spontaneous discharge (or voltage-clamped), and presynaptic spikes were elicited by brief current injection. Monosynaptic connections were identified in 14% of attempts. PC-PC connections were shown to be GABAergic, as postsynaptic responses were blocked completely and reversibly by the $GABA_A$ antagonist SR95531 (n=5). The average peak amplitude of the connections was 2.8 ± 1.2 mV (n=6), or 92.4 ± 16.1 pA (n=5) for I-Clamp and V-clamp recordings, respectively. The 20-80% rise time of the postsynaptic response was 3.9 ± 0.4 ms for I-clamp, and 0.78 ± 0.18 ms for V-clamp recordings. High-frequency presynaptic spike-trains between 10-100 Hz revealed strongly depressing synapses. Neurons were filled with biocytin for anatomical reconstructions using light microscopy. Putative synaptic contacts were predominantly somatic, with an average of 13.2 ± 2.5 putative synaptic contacts per connection (n=5). Since PCs are the sole output of the cerebellar cortex, the existence of monosynaptic PC-PC connections is likely to have important computational implications for cerebellar function, and may play a role in gain control and synchronization of the cerebellar circuit (3).

Ramón y Cajal S (1911). Histologie du Système Nerveux de l'Homme et des Vertebrés. Malone, Paris.

Eilers J, Plant TD, Marandi N & Konnerth A (2001). J Physiol 536, 429-437.

Maex R & De Schutter E (2003). J Neurosci 23, 10503-10514.

Supported by grants from EMBO (A.J.W.), the EU (P.J.S.), the Wellcome Trust and Gatsby Foundation (M.H.). L7-tau-GFP mice were a generous gift from S. du Lac. GAD65-GFP mice were a generous gift from G. Szabo and F. Erdelji.

Where applicable, the authors confirm that the experiments described here conform with the Physiological Society ethical requirements.

C109

Rundown and inhibition of oligodendrocyte NMDA receptors

Y. Bakiri, N.B. Hamilton, R. Káradóttir and D. Attwell

Physiology, UCL, London, UK

Pathologies such as cerebral palsy, spinal cord injury and multiple sclerosis involve glutamate-mediated damage to the white matter. We have recently shown that oligodendrocytes in the white matter of the cerebellum and corpus callosum express NMDA receptors, which are activated during

ischaemic conditions (Káradóttir et al. 2005). Thus, as in neurons, these receptors may cause cell damage by glutamate-induced excitotoxicity. The aim of this study was to investigate further the properties of oligodendrocyte NMDA receptors, using whole-cell voltage-clamp recordings *in situ* in rat brain slices.

Mature oligodendrocytes were whole-cell clamped with internal solution containing Cs^+ as the main cation and identified by their morphology as visualized by dye filling (Káradóttir et al. 2005). The peak current response evoked at -60mV by repetitive NMDA applications (60μM, once every ten minutes) exhibited a run-down, both in the corpus callosum and cerebellum. This run-down was area-dependent: in cerebellum the response to the third NMDA application was 33±5% (mean±s.e.m., n=13 cells) smaller than the first response, whereas in the corpus callosum it was 79±9% smaller (n=15; significantly different, p=0.0002 by 2-tailed t test). In neurons, NMDA response rundown can be reduced or abolished by lowering the extracellular calcium concentration (Rosenmund & Westbrook, 1993). However, in cerebellar oligodendrocytes, the rundown was larger when we decreased the extracellular calcium concentration from 2.5mM to 0.2mM (in 0.2mM $[Ca^{2+}]$ the response to the third NMDA application was 63±4% (n=8) smaller than the first one; significantly different to 2.5mM $[Ca^{2+}]$, p=0.0002 by 2-tailed t test). NMDA receptor blockers have been widely tested as agents that may prevent grey matter damage in conditions like stroke. The discovery of NMDA receptors in oligodendrocytes (Káradóttir et al. 2005) suggests that these blockers may be useful for treating white matter diseases. Memantine, the only clinically-approved NMDA receptor antagonist, inhibited the NMDA-evoked current in cerebellar oligodendrocytes (IC_{50}=26±7μM, 122 cells).

These data suggest that the NMDA receptors (or their downstream signalling) in oligodendrocytes differ from those in neurons and differ between white matter areas. Memantine or related compounds might be useful as a therapy for preventing white matter damage.

Káradóttir R, Cavelier P, Bergersen L & Attwell D (2005). Nature 438, 1162-1166.

Rosenmund C & Westbrook GL (1993). J Physiol 470, 705-729.

Supported by the Wellcome Trust.

Where applicable, the authors confirm that the experiments described here conform with the Physiological Society ethical requirements.

C110

Putative mossy fibre input resets spontaneous Golgi cell firing with high efficacy

R.T. Kanichay and R.A. Silver

Physiology, UCL, London, UK

Inhibition of cerebellar granule cells (GrCs) by Golgi cells (GoCs) is thought to be important for cerebellar information processing (Marr, 1969; Wantanabe et al. 1999). GoCs receive excitatory input from mossy fibres (MFs) and parallel fibres, an anatomical arrangement that provides both feed-forward and feed-back inhibition onto GrCs. We have investigated the properties of putative MF synaptic connections onto GoCs and examined their impact on GoC firing.

Excitatory postsynaptic currents (EPSCs) evoked with white matter stimulation were recorded using whole-cell voltage-clamp recording of GoCs in cerebellar slices from p25 rats at 35°C. EPSCs evoked with minimal stimulation had fast kinetics (10-90% rise time=0.3±0.1ms; 37% decay time=0.9±0.4ms) and a mean amplitude of 57±25pA with high variability (CV=0.72; n=18). The short response latency (0.8±0.2ms), pharmacological profile and absence of pronounced short-term plasticity suggest that EPSCs result from MF stimulation.

To examine the role of the putative MF input, we recorded GoC firing in response to MF tract stimulation in loose cell-attached patch mode. GoCs were spontaneously active at 9±4Hz. Single-pulse MF tract stimulation elicited an action potential (AP), that reset the phase of spontaneous GoC firing. Subsequent whole-cell recordings at the same stimulus intensity revealed that the synaptic current underlying AP generation was 230±110pA; n=5. This suggests that simultaneous activation of a few MFs is sufficient to reset GoC firing.

Our data provide information on the properties of the previously uncharacterized MF-GoC synaptic connection and suggests that MFs have a high efficacy in driving GoC firing. Our results suggest that simultaneous activation of few MFs can influence the timing of inhibition onto the ~5000 GrCs innervated by a single GoC axon (Pellionisz and Szentagothai in Ito 1984). This feed-forward inhibition therefore is likely to play an important role in signal processing in the granule cell layer by synchronizing the time window of synaptic integration in granule cells.

Marr (1969). J Physiol 202, 437-470.

Wantanabe et al. (1999). Cell 95, 17-27.

Pellionisz & Szentagothai (in Ito) (1984). The Cerebellum and Neural Control. Raven Press, New York.

Funded by the Wellcome Trust, MRC and EC.

Where applicable, the authors confirm that the experiments described here conform with the Physiological Society ethical requirements.

PC139

Modulation of neuronal nicotinic receptors in rat intrinsic cardiac ganglia by non-depolarizing muscle relaxants

D.J. Adams and R. Kanjhan

School of Biomedical Sciences, University of Queensland, Brisbane, QLD, Australia

Non-depolarizing neuromuscular blocking drugs such as tubocurarine, pancuronium and vecuronium, are potent inhibitors of muscle nicotinic acetylcholine receptors (nAChRs) and are commonly used as muscle relaxants during abdominal surgery. Previous studies have reported adverse effects of these drugs on heart rate and other cardiovascular parameters (Son & Waud, 1980; Narita *et al.* 1992). The effects of muscle relaxants on neuronal nAChRs were investigated in dissociated neurons from rat (5-14 days old) intracardiac ganglia (ICG), which mediate vagal parasympathetic control of the heart. Amphotericin B perforated-patch clamp technique was employed to determine firing properties of ICG neurons and their response to 3 s rapid, focal application of nicotine alone (100 μM) or together with vecuronium, tubocurarine or pancuronium. There was significant variation in peak amplitude, time course and recovery of nicotine-evoked responses among ICG neurons. The mean peak amplitude of nicotine-evoked inward currents at -60 mV was significantly larger (approximately 4-fold) in neurons exhibiting tonic (-26.4 pA/pF; n=6) and accommodating (-25.8 pA/pF; n=6) firing patterns compared to phasic (-6.9 pA/pF; n=17; $P < 0.0001$). Vecuronium, tubocurarine and pancuronium at 1 μM inhibited nicotine-evoked currents by 80%, 55% and 37% with approximate IC_{50} values of 0.9, 9.6 and 100 nM, respectively. Pancuronium modulation of nicotine-evoked currents was biphasic in 7 of 11 neurons tested whereby potentiation was observed at low concentrations (<10 nM) and inhibition at higher concentrations with maximum inhibition of 40% at 10 μM. Concentration-response curves of inhibition by muscle relaxants were shifted left by ~10-fold in tonic or accommodating neurons compared to the phasic neurons. Taken together, these data indicate that nAChR-mediated currents in ICG neurons and their modulation by muscle relaxants are closely correlated with neuronal firing patterns.

Son SL & Waud DR (1980). *Br J Anaesth* **52**, 981-987.

Narita M *et al.* (1992). *J Pharmacol & Exp Ther* **262**, 577-583.

Where applicable, the authors confirm that the experiments described here conform with the Physiological Society ethical requirements.

PC140

Inhibition of production of amyloid beta$_{1-40}$, but not amyloid beta$_{1-42}$, results in decreased viability in the SH-SY5Y neuroblastoma cell line and in primary cortical neurones

J.M. Edwards[1], C. Peers[2] and H.A. Pearson[1]

[1]Institute of Membrane and Systems Biology, University of Leeds, Leeds, UK and [2]Institute for Cardiovascular Research, University of Leeds, Leeds, UK

The γ-secretase enzyme complex is responsible for the cleavage of amyloid precursor protein (APP) to form the 40 or 42 amino acid amyloid beta protein (Aβ). Inhibition of γ-secretase has been suggested as a potential therapy in Alzheimer's disease however we have previously shown that inhibition of this enzyme complex can be toxic, resulting in a 60% loss of viability in primary neuronal cultures and neurone-like cell lines (Plant *et al.* 2003). In this study we have used three inhibitors of γ-secretase which differentially decrease production of the two size forms of amyloid beta protein and have investigated the resulting effects on cell viability.

Dissociated cultures of cortical neurones were prepared from 1 day old rats and maintained as reported previously (Plant *et al.* 2005). SH-SY5Y cells were cultured as reported previously (Plant *et al.* 2005). Data are presented as mean ±S.E.M and statistical differences were assessed using Student's t test.

Human neuroblastoma SH-SY5Y cells and primary cortical neurones were incubated with 10μM γ-secretase inhibitor for 24 hours. Preferential inhibition of release of $A\beta_{1-40}$, using γ-secretase inhibitor I, resulted in a 56.5±5.3% (n=7, $P<0.001$) reduction in viability in SH-SY5Y cells and a 29±15% (n=3) reduction in cell viability in primary cortical neurones as measured using a Live/Dead cytotoxicity assay kit. Selective inhibition of production of the 42 amino acid isoform, using γ-secretase inhibitor VI, had no significant effect on viability in either cell type. Inhibition of release of both peptides concurrently by γ-secretase inhibitor IV resulted in an 8.8±3.2% decrease in viability (n=13, $P<0.05$) in SH-SY5Y cells and a 15.0±4.9% decrease in viability of cortical neurones (n=3).

Co-incubation of cells with 1nM $A\beta_{1-40}$ partially reversed the effects of inhibiting production of $A\beta_{1-40}$ (12.8±14.0% increase in viability, n=6) and completely reversed the toxicity associated with preventing production of $A\beta_{1-40}$ and $A\beta_{1-42}$ concurrently (viability returned to 99.7±0.5%, $P<0.001$, n=6). Enhanced differentiation of SH SY5Y cells by exposure to 10μM retinoic acid for 7 days resulted in exaggerated responses to the secretase inhibitors (n=2).

These findings demonstrate that inhibition of production of amyloid beta $_{1-40}$ but not $_{1-42}$ is detrimental to cells suggesting a pivotal role of amyloid beta $_{1-40}$ in normal neuronal physiology.

Plant LD *et al.* (2003). *J Neurosci* 23, 5531-5535.

Plant LD *et al.* (2005). *Neurobiol Aging* (in press).

J.M.E. is funded by an Emma and Leslie Reid Scholarship.

Work in the laboratory is funded by the MRC and Alzheimer's Research Trust.

Where applicable, the authors confirm that the experiments described here conform with the Physiological Society ethical requirements.

PC142

Physiological mechanisms of lysophosphatidylcholine-induced interleukin-1β release from brain macrophages

T. Schilling[1], C. Stock[2], A. Schwab[2] and C. Eder[1]

[1]Institute of Physiology, Berlin, Germany and [2]Institute of Physiology II, Muenster, Germany

Release of interleukin-1β (IL-1b) represents one of the earliest responses of brain macrophages (microglia) to brain injury and

IL-1b itself contributes to brain damage (Allan et al. 2005). Stimulation of the murine microglia cell line BV-2 with lysophosphatidylcholine (LPC) caused rapid IL-1b release that occurred independently of P2X7 ATP receptor activation. Neither LPC-induced IL-1b release (n=3 experiments) nor LPC-stimulated intracellular Ca^{2+} increases (n=144 cells) were affected by inhibition of P2X7 ATP receptors with 500 μM oxidized ATP. Patch-clamp experiments revealed activation of non-selective cation currents and Ca^{2+}-dependent K^+ currents by 15 μM extracellular LPC. LPC-activated non-selective cation channels were permeable for monovalent and divalent cations. They were inhibited by 100 μM Gd^{3+} (n=11 cells), 100 μM La^{3+} (n=10 cells), 500 μM Zn^{2+} (n=4 cells) and Grammostola spatulata venom (diluted 1:2000; n=7 cells), but were unaffected by 100 μM diltiazem (n=7 cells), 50 μM LOE908MS (n=7 cells), 1 mM amiloride (n=7 cells) and 200 μM DIDS (n=7 cells). Ca^{2+} influx through non-selective cation channels was sufficient to elicit charybdotoxin (CTX)-sensitive Ca^{2+}-dependent K^+ currents (n=21 cells). Microglial IL-1b release was suppressed in Ca^{2+}-free extracellular medium (n=4 experiments; $p<0.001$) or during inhibition of non-selective cation channels with Gd^{3+} or La^{3+} (n=4 experiments for each condition; $p<0.001$). It was also attenuated in the presence of 200 nM CTX (n=4 experiments; $p<0.05$), but was unaffected by margatoxin (n=3 experiments), suggesting that Ca^{2+}-activated K^+ channels rather than voltage-activated K^+ channels are important for microglial IL-1b release. The K^+ ionophore nigericin (10 μM) did not reverse suppressive effects of CTX on LPC-stimulated IL-1b release, demonstrating the importance of membrane hyperpolarization. In all experiments, the statistical significance of differences between experimental groups was evaluated by the Mann-Whitney U test.

In summary, these data indicate that LPC-stimulated IL-1b release from microglia is a Ca^{2+}- and voltage-dependent process. Inhibitors of non-selective cation channels and Ca^{2+}-activated K^+ channels may represent tools for IL-1b inhibition during neuroinflammatory and neurodegenerative diseases.

Allan SM, Tyrrell PJ & Rothwell NJ (2005). Nat Rev Immunol 5, 629-640.

This work was supported by the Deutsche Forschungsgemeinschaft: grant SFB 507/C7 (to C.E.) and grant Schw 407/9-1,2 (to A.S.).

Where applicable, the authors confirm that the experiments described here conform with the Physiological Society ethical requirements.

PC143

Dendritic spikes impose a frequency limit on somatic simple spikes in cerebellar Purkinje neurons

E.A. Rancz and M. Häusser

Department of Physiology and Wolfson Institute for Biomedical Research, University College London, London, UK

Dendritic spikes enhance the somatic spike output of many neuron types. This is usually manifested by an increase in the number of spikes (transition to bursting, increase in gain) or in an increase in the precision of the spikes for a given input. We have examined the effect of dendritic spikes on spike output in Purkinje cells using simultaneous somatic and dendritic patch-clamp recordings in slices taken from P18–26 rats maintained at 34°C. Stimulation of parallel fibres triggered dendritic calcium spikes which acted to brake somatic firing: as the synaptic stimulation intensity was increased, calcium spikes caused a decrease in somatic output frequency in response to the stimulus, attaining a maximum average firing rate of 214 ± 8 Hz (n = 5) which became independent of the strength of synaptic input. To investigate this effect, synaptic-like current waveforms were injected into the dendrite (>100 μm from the soma) and the somatic spike output was measured. Increasing the injected current resulted in a linear increase in the average somatic sodium spike output (r = 0.98 ± 0.01, slope = 313 ± 35 Hz/nA, n = 5) until the point where dendritic spikes appeared. Increasing the injected current further did not increase the average somatic spike output (r = -0.081 ± 0.2, slope = -17 ± 12 Hz/nA, n = 5, $p < 0.005$ vs. no dendritic spikes). Dendritic spikes effectively clamped the average somatic output at a rate of 214 ± 16 Hz (n = 5), while permitting fast doublets with a maximal instantaneous firing rate of 461 ± 81 Hz. Penitrem A (100 nM), a large-conductance calcium-activated potassium (BK) channel blocker, rescued the monotonically-increasing f/I relationship when dendritic spikes were evoked (r = 0.78 ± 0.12, slope = 187 ± 57 Hz/nA, n = 3, $p > 0.2$) without changing the slope of the sub-dendritic spike regime (r = 0.93 ± 0.04, slope = 308 ± 43 Hz/nA, n = 3, $p > 0.9$ vs. control). The maximum sustained spike rate reached 290 Hz while the maximum instantaneous spike rate exceeded 650 Hz in penitrem A. Interestingly, both the maximum sustained and instantaneous firing rates under control conditions are comparable to the frequency limit of axonal propagation (1,2), while during BK channel block the somatic spike rates could exceed this limit. Dendritic spikes in Purkinje cells, in contrast to many other neuronal types, therefore clamp the average somatic spike output of Purkinje cells at a rate that ensures that parallel fibre-evoked simple spikes will propagate down the axon. Statistical significance was assessed by Student's t test, and all data are given as average ± SEM.

Khaliq ZM & Raman IM (2005). J Neurosci **25**, 454-463.

Monsivais P et al. (2005). J Neurosci **25**, 464-472.

Supported by The Wellcome Trust.

Where applicable, the authors confirm that the experiments described here conform with the Physiological Society ethical requirements.

PC144

A reduction in the frequency and amplitude of spontaneous mIPSCs in dystrophin-deficient *mdx* mice

S.I. Head, S.L. Kueh and J.W. Morley

Physiology & Pharmacology, University of New South Wales, Sydney, NSW, Australia

Duchenne muscular dystrophy (DMD) is the second most common single gene disorder in humans, affecting 1 in 3500 live male births (1). It results from mutation in the dystrophin gene causing the absence of the normal full length dystrophin product (2). Apart from its symptoms of muscle wasting, a significant cognitive impairment has also been reported in DMD patients (3,4). Here, we investigate the effect of the absence of dystrophin on

the frequency and amplitude of spontaneous miniature inhibitory postsynaptic currents (mIPSCs) in cerebellar Purkinje cells of the dystrophin-deficient *mdx* mouse compared to littermate controls. Whole-cell patch-clamp recordings from Purkinje cells were performed in saggital cerebellar slices from *mdx* (n = 7) and littermate control (n = 6). Purkinje cells were held at -80mV and to prevent action potential-evoked events, TTX (1μM) was added to the bathing solution (composition in mM: NaCl 124, KCl 3.2, $CaCl_2$ 2.5, $MgCl_2$ 1.3, $NaHCO_3$ 26, NaH_2PO_4 1.25 and D-glucose 25; bubbled with 95% O_2 and 5% CO_2). Spontaneous mIPSCs were analysed using MiniAnalysis (Synaptosoft), for details of the experimental protocol see (5). We found a significant difference (all errors are expressed as SEM) between the frequency of spontaneous mIPSCs in *mdx* (1.38 ± 0.46 Hz; n = 8 cells) and littermate control mice (2.74 ± 1.00 Hz; n = 8 cells) (two-tailed t test, p = 0.0036). The average amplitude of mIPSCs from littermate controls (74.81 ± 7.840 pA, n=9) were also significantly different from *mdx* mice (53.81 ± 4.621 pA, n=8), p = 0.041, two tailed unpaired t test. The reduction in the frequency and amplitude of mIPSCs in dystrophin deficient mice could be due to a mislocalization of the $GABA_A$ receptor channels at post-synaptic regions. This finding suggests that dystrophin may play an important role in ion channel localization in cerebellar Purkinje cells.

Emery AH (1991). Neuromuscul Disord 1, 19-29.

Hoffman EP et al. (1987). Cell 51, 919-928.

Bresolin N et al. (1994). Neuromuscul Disord 4, 359-369.

Anderson JL et al. (2002). Brain 125, 4-13.

Anderson JL et al. (2003). Brain Res 982, 280-283.

Supported by the Muscular Dystrophy Association (USA).

Where applicable, the authors confirm that the experiments described here conform with the Physiological Society ethical requirements.

PC145

Development of feedforward inhibition in rodent barrel cortex

M. Daw[1] and J.T. Isaac[2]

[1]MRC Centre for Synaptic Plasticity, University of Bristol, Bristol, UK and [2]NINDS, NIH, Bethesda, MD, USA

Feedforward inhibition mediated by $GABA_A$ receptors has been shown to regulate the timing of postsynaptic action potentials in layer 4 cells of rodent somatosensory (barrel) cortex (Gabernet et al. 2005). However, the role of immature GABAergic transmission, which is widely reported to be depolarising (Ben-Ari, 2002), has not been investigated. We have used gramicidin perforated patch-clamp recordings from layer 4 cells in mouse thalamocortical (TC) slices to measure the reversal potential of pharmacologically isolated $GABA_A$-mediated currents during development from postnatal day (P) 3-P9. The reversal potential over this period changed from -53 ± 3 mV (P3, n = 3) to -71 ± 2 mV (P9, n = 3). We also used whole cell recordings to measure the relative contributions of $GABA_A$ and glutamate receptors to TC synaptic currents over the same age range. The contribution of $GABA_A$ receptors increased greatly with age ($GABA_A$ charge transfer as a percentage of glutamate receptor-mediated charge: P4 = 10 ± 6%, n = 10; P9 = 343 ± 93%, n = 8, $p < 0.001$ (unpaired t test). In the same cells the latency of the peak $GABA_A$-mediated synaptic response decreased (latency from stimulus: P4 = 47 ± 30 ms, P9= 5 ± 1 ms, p < 1 x 10-4), as did the variability in this latency (S.D. of latency: P4 = 22 ± 6 ms, P9 = 0.9 ± 0.4 ms; $p < 1 \times 10^{-5}$). Thus GABAergic transmission shows a profound change in its properties during the first postnatal week. To investigate the consequences of this, we studied the effects of feedforward GABAergic transmission on action potentials evoked by TC input using perforated patch recordings. In P3-5 animals application of the $GABA_A$ antagonist, bicuculline methobromide (BMB) had no effect on the probability or latency of action potential firing (probability: control 34 ± 5%, BMB 34 ± 10%, n = 7, p = 1; latency: control 12 ± 2, BMB 14 ± 2 ms, n = 5, p = 0.3). In P8-9 animals application of BMB caused an increase in firing probability (control = 31 ± 7%, BMB = 89 ± 6%, n = 14, p < 1 x 10-5 paired t test) but had no effect on action potential timing (latency: control = 5 ± 1 ms, BMB = 6 ± 1 ms, n = 10, p = 0.5; jitter (S.D. of latency): control = 2 ± 1 ms, BMB = 2 ± 1 ms, n = 10, p = 0.8). However, when stimulus intensity was decreased in the presence of BMB to return firing probability to baseline values a robust change in action potential timing was observed (latency: control = 5 ± 1 ms, BMB = 10 ± 1 ms, n = 5; p < 0.01, jitter: control = 1 ± 1 ms, BMB = 4 ± 1 ms, n = 5, p < 0.05). Our findings demonstrate a dramatic functional switch in the role of GABAergic input to layer IV barrel cortex during development. Moreover, our data indicate that mature, hyperpolarising GABAergic transmission, rather than causing high timing fidelity of action potential timing per se, also restricts action potential firing only to synaptic input of sufficient amplitude to result in high timing precision.

Ben-Ari Y (2002). Nat Rev Neurosci 3, 728-739.

Gabernet L, Jadhav SP, Feldman DE, Carandini M & Scanziani M (2005). Neuron 48, 315-327.

Where applicable, the authors confirm that the experiments described here conform with the Physiological Society ethical requirements.

PC146

Confocal measurements of intracellular Ca^{2+} changes in axonal varicosities of noradrenergic neurones in slice cultures of the medulla oblongata

A.G. Teschemacher[1], Z. Chiti[1], J.F.R. Paton[2] and S. Kasparov[2]

[1]Department of Pharmacology, Bristol Heart Institute, School of Medical Sciences, University of Bristol, Bristol, UK and [2]Department of Physiology, Bristol Heart Institute, School of Medical Sciences, University of Bristol, Bristol, UK

One role of noradrenergic (NAergic) neurotransmission in the medulla oblongata is in the regulation of arterial pressure (Reis et al. 1977; Duale et al. 2005). In order to gain a better understanding of the mechanisms regulating central noradrenaline (NA) release, we imaged intracellular Ca^{2+} signalling in NAergic axonal varicosities of A1 and A2 neurones.

Organotypic rat brainstem slice cultures were transfected with adenoviral vectors driving expression of enhanced green fluorescent protein in catecholaminergic neurones specifically

(Teschemacher et al. 2005a). Green fluorescent NAergic neurones were visualised (excitation 488, emission 500-530 nm) by combined upright confocal and DIC optics on a Leica SP2 system. Axonal varicosities (diameters ~2-4 μm) were evident on axonal branches several hundred micrometers from their cell body. This distance precluded adequate filling with a fluorescent Ca^{2+} indicator loaded from a patch electrode located at the soma (Teschemacher et al. 2005b). Therefore, we patched varicosities directly and loaded them with the Ca^{2+}-sensitive dye Rhod-2 (0.5 mM) contained in the pipette solution. Changes in their intracellular Ca^{2+} concentration were monitored by confocal fluorescence imaging (excitation 543 nm, emission 560-630 nm) in XY-t mode (at ~ 15 Hz) or in X-t line scan mode (at ≤ 1 ms/line). We found that adjacent varicosities were loaded successfully after patching a single varicosity. Electrical recording duration was variable (10-60 min). With good electrical access, action potentials were triggered by injection of current through the patch pipette. In the absence of electrical access, the axon was stimulated electrically via an extracellular microelectrode. Both modes of electrical stimulation evoked Ca^{2+} transients. In addition, Ca^{2+} transients also occurred spontaneously without evidence of action potentials.
In conclusion, we have developed an approach for imaging Ca^{2+} transients in NAergic axonal varicosities. The finding of action potential-independent Ca^{2+} transients suggests the local activation of metabotropic receptors which may mediate Ca^{2+} release from intracellular stores in varicosities.

Duale H, Teschemacher AG, Waki H, Kasparov S & Paton JF (2005). J Physiol 567P, PC39.

Reis DJ, Doba N, Snyder DW & Nathan MA (1977). Prog Brain Res 47, 169-188.

Teschemacher AG, Wang S, Lonergan T, Duale H, Waki H, Paton JF & Kasparov S (2005a). Exp Physiol 90, 61-69.

Teschemacher AG, Wang S, Paton JF & Kasparov S (2005b). J Physiol 567P, PD1.

This work was supported by the British Heart Foundation, the Wellcome Trust, and the Royal Society. Z.C. was in receipt of a Wellcome Trust-University of Bristol Value-in-People award.

Where applicable, the authors confirm that the experiments described here conform with the Physiological Society ethical requirements.

PC148

Frequency and timing dependence of spike timing-dependent plasticity in the hippocampus

K.A. Buchanan and J. Mellor

MRC Centre for Synaptic Plasticity, University of Bristol, Bristol, UK

Spike timing-dependent plasticity (STDP) of synaptic strength is thought to require the coincidence of presynaptic glutamate release and postsynaptic depolarisation through back propagating action potentials (Magee & Johnston, 1997; Markram et al. 1997). The exact timing of these presynaptic and postsynaptic spikes has been shown to dictate the direction and magnitude of the resulting plasticity at a variety of different synapses. However, evidence for this phenomenon in acute hippocampal slices is less clear. There is also evidence that modulatory inputs to the hippocampus, such as acetylcholine (ACh), can alter the behaviour of back propagating action potentials (Tsubokawa & Ross, 1997). Therefore we examined if ACh can modulate STDP in the hippocampus.
Hippocampal slices (300-400μm) were prepared from 2 week old male Wistar rats and whole cell patch clamp recordings made from visualised CA1 pyramidal neurones at room temperature (23°C) in the presence of 50μM picrotoxin. In voltage clamp, baseline EPSCs from 2 independent pathways were elicited by stimulation in stratum radiatum at 0.1Hz. In current clamp, synaptic plasticity was induced by 4 trains of 100 stimuli given at 1 min intervals to the proximal pathway. Each stimulus consisted of a presynaptic input coupled with a postsynaptic action potential induced by a 2ms 0.5A current injection. The spike timing interval (STI) between the presynaptic and postsynaptic event in each stimulus was measured as the difference between the onset of the EPSP and the peak of the action potential. The EPSC amplitude in both pathways was then monitored for a further 30min. Pairs of presynaptic and postsynaptic spikes with a STI of +6 to +13ms were able to induce homosynaptic LTP when the stimuli were delivered at 20Hz (140±17%, n=11, $p<0.05$) or 10Hz, (146±20%, n=4, $p<0.05$) but not at 5Hz (113±18%, n=8, p=0.5) or 1Hz (95±21%, n=4, p=0.8) thus demonstrating the frequency dependence of STDP. Changing the timing of the stimuli given at 10Hz also altered synaptic plasticity. STIs of +6.2ms to +13ms resulted in potentiation whereas STIs of +2.5ms to +6.2ms resulted in a small non-significant depression (76±45%, n=6, p=0.3). When stimuli with STI values of +8-13ms were delivered at 10Hz in the presence of 1μM carbachol, the ACh receptor agonist, the synaptic potentiation seen in the absence of carbachol was blocked (96±19%, n=8, p=0.8). All statistical values shown are paired Student's t tests. These results demonstrate that STDP in acute hippocampal slices is frequency and timing dependent requiring stimuli repeated at 10Hz or more with STIs between +6.2 and +13ms. We also show that STDP is inhibited by activation of ACh receptors. This is contrary to reports that activation of ACh receptors generally increases the excitability of CA1 pyramidal neurons and increases the back propagation of action potentials.

Magee & Johnston (1997). Science 275, 209-213.

Markram et al. (1997). Science 275, 213-215.

Tsubokawa & Ross (1997). J Neurosci 17, 5782-5791.

GSK funded PhD Studentship.

Where applicable, the authors confirm that the experiments described here conform with the Physiological Society ethical requirements.

PC149

Inward currents elicited by metabolic inhibition in rat dorsal vagal neurones

R.H. Balfour and S. Trapp

Dept of Anaesthetics, Pain Medicine & Intensive Care, Imperial College London, London, UK

A proportion of dorsal vagal neurones (DVN) have been shown to respond to metabolic inhibition (MI) with a K_{ATP} channel-mediated outward current [1,2]. Here we show that MI also elicits small inward currents in DVN.
Brainstem slices (200 μm) were obtained from juvenile Sprague-Dawley rats. After 30min recovery at 34°C, slices were kept at 22°C

in artificial cerebrospinal fluid (ACSF). Whole-cell recordings were used to assess the response to metabolic inhibition elicited by bath application of either 1 mM cyanide (1-3 min), 3 mM azide (1-3 min) or glucose-free ACSF (hypoglycaemia; 5-30 min).
MI-induced a K_{ATP} channel-mediated outward current in 16 DVN [see 1,2]. Prior to the development of the K_{ATP} current, an inward current was observed. This current was also seen in 45 neurones without functional K_{ATP} channels. It was small (-30±3 pA at –70 mV holding potential; mean ± 1 s.e.m.; n=24) with a fast onset (90±4 s; n=40) for azide and cyanide. In contrast, for hypoglycaemia the onset was 184±48 s (n=4) in non-glucose-sensors and 38±11 s (n=3) in glucose-sensors [2].
Analysis of the current-voltage relations revealed that MI induced a decrease of conductance in some DVN. This conductance had a reversal potential (Rev) close to E_K (-95±4 mV; n=5) and was well described by the Goldman-Hodgkin-Katz equation, indicating an openly rectifying K^+ channel. In the remaining cells MI led to an increase in conductance with a Rev between -65 and 10 mV; n=24). An inward current of -17±4 pA at -70 mV pA, onset of 100±20 s, (n=3) with Revs of -30, -45 and -100 mV was seen in response to MI in 0 mM $[Ca^{2+}]_o$. Using 143 mM instead of 5 mM $[Cl^-]_i$ an inward current of -18±4 pA at -70 mV with an onset of 100±27 s and Revs of -25, -50 and of -92 mV, was elicted by MI.
Na^+/K^+ ATPase inhibition (100 μM strophanthidin or 50 μM ouabain) produced an inward current of -43±6 pA at -70 mV (n=7). The amplitude of this current was not significantly different from that elicited by MI (paired t test, $p>0.05$). However, the current induced by Na^+/K^+ ATPase inhibition showed no Rev within -20 to -120 mV.
In summary, DVN responded to MI either with a decrease of an openly rectifying K^+ conductance or an increase in conductance, which was not mediated by Cl^- or Ca^{2+}, but may be due in part to inhibition of the Na^+/K^+ ATPase. The onset of current in response to mitochondrial inhibition was significantly faster ($p<0.01$) than in response to hypoglycaemia and glucose-sensors responded much faster than non-glucose-sensors. These results suggest that glucose-sensors are more sensitive to MI and that $[ATP]_i$ is the key mediator for the electrical responses.

Trapp & Ballanyi (1995). J Physiol 487, 37-50.

Balfour et al (2006). J Physiol 570, 469-484.

This work was supported by an MRC Career Development Award to S.T.

Where applicable, the authors confirm that the experiments described here conform with the Physiological Society ethical requirements.

PC150

Whole-cell recording of neuronal populations in the inferior colliculus of the adult guinea pig

J. Navarro-Lopez and J. Ashmore

Physiology, UCL, London, UK

The inferior colliculus (IC) receives projections from different sources within the auditory system and processes information ascending from the periphery and to send it forward to cortical structures. The activity pattern of each IC neuron depends on brainstem input and, at least in part, its physiological state and on the types of ionic currents patterning intrinsic discharge patterns. In vitro recording from early stage animals makes the case that voltage-gated K channels underlie the distinct IC neuronals discharge patterns observed (Sivaramakrishnan & Oliver, 2001). However it is clear that maturation of auditory neurons may change channel density (Koch & Grothe, 2003) and auditory-pathway specific K channels may also alter in expression during development (Kharkovets et al. 2000).
We have attempted to determine how the presence of voltage-gated K channels contributes IC neuronal firing pattern and synaptic responses in mature animals. 300 μm thick coronal brainstem slices were made from tissue from guinea pigs (250-300g) which included both inferior colliculi. Slices were sectioned in cold ACSF (in mM: 117 NaCl, 4.7 KCl, 2.5 $CaCl_2$, 1.2 $MgCl_2$, 25 $NaHCO_3$, 1.2 NaH_2PO_4, and 11 glucose) and maintained in an incubation chamber at room temperature for 2 h. Slices containing the rostral IC were placed in a recording chamber and superfused with oxygenated ACSF at room temperature. Whole-cell patch-clamp recordings were performed under visual control with a pipette containing in mM: 120 K-gluconate, 5 NaCl, 11 EGTA, 1 $CaCl_2$, 3 Mg-ATP, and 0.3 GTP-Tris, and 10 HEPES, pH 7.3, 300-310 mOsm). The recordings revealed at least three different types of neurons according to firing patterns and current-voltage relationships. Neurons were in addition stained with Alexa 488 in the patch pipette and their morphology reconstructed using confocal microscopy. The largest group of IC neurons recorded was 'onset pattern', firing only once to depolarizing current injection and/or once after a hyperpolarizing pulse. Their resting membrane potential was -57 ± 2 mV and the input resistance 98 ± 10 MΩ (mean± SD, n=8), with prominent outward rectification above -40 mV. Approximately 25% of this outward current was sensitive to perfusion with linopirdine (20 μM) a blocker of the Kv7 family of K channels. A smaller sample of cells although also classified as 'onset pattern' exhibited in addition an inward current at negative potentials. This population had a resting membrane potential of 52 ± 2 mV and an input resistance of 55 ± 11 MΩ (n=5). These results show that it is feasible to record properties of adult neuronal cells which underlie the response patterns of cells recorded in the whole animal.

Kharkovets T, Hardelin JP, Safieddine S, Schweizer M, El-Amraoui A, Petit C & Jentsch TJ (2000). Proc Natl Acad Sci U S A 97, 4333-4338.

Koch U & Grothe B (2001). J Neurophysiol 90, 3679-3687.

Sivaramakrishnan S & Oliver DL (2001). J Neurosci 21, 2861-2877.

Supported by the Wellcome Trust.

Where applicable, the authors confirm that the experiments described here conform with the Physiological Society ethical requirements.

PC151

Selective ablation of the $GABA_A$ receptor γ2 subunit from cerebellar Purkinje cells of mice eliminates IPSCs and alters simple spike timing

P. Wulff[1], M. Renzi[2], D.A. Andersson[2], L. Kelly[2], W. Wisden[3] and M. Farrant[2]

[1]Clinical Neurobiology, University of Heidelberg, Heidelberg, Germany, [2]Pharmacology, UCL, London, UK and [3]Institute of Medical Sciences, University of Aberdeen, Aberdeen, UK

Cerebellar Purkinje cells receive GABA-mediated feed-forward inhibitory input from molecular layer interneurons (MLINs; stellate and basket cells) that is thought critical for the precise timing of parallel-fibre evoked action potentials (1). Purkinje cells express mainly α1, β2 and γ2 subunits of the $GABA_A$ receptor and the γ2 subunit is likely responsible for clustering of $GABA_A$ receptors at synapses (2-3). As part of a strategy to use transgenic mice for the investigation of CNS function through reversible modulation of specific brain circuits (4), we selectively inactivated the γ2 subunit gene in Purkinje cells, using mice with Cre recombinase driven from the L7 promoter (L7Cre) crossed with a line harbouring a floxed γ2 subunit allele (fγ2). *In situ* hybridization on brain sections with an exon 4-specific probe confirmed the selective absence of γ2 subunit mRNA from L7Cre x fγ2/fγ2 Purkinje cells.

We made recordings from Purkinje cells in acute cerebellar slices from L7Cre x fγ2/fγ2 mice and their WT littermates. Mice were anaesthetised prior to decapitation. Responses to exogenous GABA were observed in patches taken from Purkinje cells of both groups of mice. Consistent with the loss of a γ2 subunit, currents recorded from L7Cre x fγ2/fγ2 mice showed a lower single-channel conductance and incomplete desensitization. Purkinje cell miniature IPSCs (mIPSCs) were observed in all WT mice, but in no L7Cre x fγ2/fγ2 mice. In accord with the Purkinje cell-selective expression of Cre, MLINs from both groups displayed mIPSCs.

Purkinje cells fire simple spikes spontaneously and the activity of interneurons influences spike timing (5). Of the cells recorded, 61 of 68 fired action potentials spontaneously. The mean firing rate of Purkinje cells from the two groups was not significantly different, either at room- or physiological temperature. However, the coefficient of variation (CV; SD/mean) of the interspike interval (ISI) differed. At 25°C the CV was 0.20 ± 0.03 for 26 cells from WT and 0.10±0.01 for 9 cells from L7Cre x fγ2/fγ2 mice (mean±sem, P<0.05, Mann-Whitney U test). At 35°C the CVs were 0.14±0.01 and 0.06±0.01, respectively (n=9 and 7, P<0.05).

Consistent with a role for MLINs in shaping Purkinje cell firing patterns (5), blockade of $GABA_A$ receptors with SR95531 decreased the CV of the ISI in WT Purkinje cells from 0.20±0.04 to 0.13±0.02 at 25°C and from 0.13±0.02 to 0.08±0.01 at 35°C (both P<0.05, paired t test; n=8 and 4, respectively). SR95531 failed to alter the CV of the ISI in cells from L7Cre x fγ2/fγ2 mice. Our results support the idea that γ2 subunits are needed for targeting of $GABA_A$ receptors to synaptic sites in Purkinje cells. We are currently investigating the behavioural outcome of this loss of normal inhibitory input.

Mittmann *et al.* (2005). J Physiol 563, 369.

Schweizer *et al.* (2003). Mol Cell Neurosci 24, 442.

Alldred *et al.* (2005). J Neurosci 25, 594.

Wulff & Wisden (2005). TINS 28, 44.

Hausser & Clark (1997). Neuron 19, 665.

Supported by: Wellcome Trust, VolkswagenStiftung and DFG.

Where applicable, the authors confirm that the experiments described here conform with the Physiological Society ethical requirements.

PC152

The effect of M-current antagonists on the electrical properties and synaptic transmission in rat intracardiac neurones *in situ*: developmental perspectives

K. Rimmer and A.A. Harper

Molecular Physiology, University of Dundee, Dundee, UK

The M-current contributes to the maintenance of resting membrane potential and underpins the adaptation properties of dissociated neonatal rat intracardiac ganglion (ICG) neurones. However, studies using rat dissociated ICG neurones have shown that the expression of the hyperpolarization-activated (I_h) and inward rectifier K^+ ($I_{K(IR)}$) currents and ATP-sensitive K^+ conductance ($I_{K(ATP)}$) all show changes during postnatal development (Adams & Cuevas, 2004).

We have used a wholemount preparation and intracellular recording techniques to investigate the action of M-current blockers on ICG neurones. Membrane potential (E_m), input resistance (R_{in}), afterhyperpolarization (AHP) amplitude and duration, and synaptic responses were measured. We studied two time points during postnatal development: neonatal (P2-5) and adult (≥ 42 days) and compared the actions of the wide-spectrum K^+ channel blocker Ba^{2+} (which at 1mM blocks the M-channel), the selective M-channel blocker linopirdine (10 μM) and the M1 muscarinic antagonist oxotremorine M (oxo-M, 10 μM). Ba^{2+} and linopirdine significantly depolarized E_m by ~6-8 mV in both neonates (n=10, p=0.003; n =3, p=0.04, paired t test) and adult ICG neurons (n=13, p=0.0003; n=4, p=0.01). Oxo-M had no significant effect on E_m. The action of these agents on R_{in} was inconsistent. Ba^{2+} produced a significant increase in R_{in} for both neonatal and ICG neurones (to 135 ± 33, and 178% ± 63 SD of control values). Linopirdine had no significant action and oxo-M increased R_{in} significantly in adult (to 134% ± 37, n=6) but not in neonatal ICG neurones.

Ba^{2+} increased the duration of the AHP and oxo-M increased the AHP amplitude in neonatal ICG neurones, linopirdine had no action on AHP parameters. Ba^{2+} and linopridine also switched evoked firing patterns. In control conditions the discharge was predominantly phasic (neonates, 77%; adults, 90%). Ba^{2+} altered discharge to multiply adapting and tonic (100 and 57% for neonates and adults, respectively). Linopirdine caused a similar shift in discharge activity. In contrast, oxo-M had little impact on discharge pattern in either neonate or adult ICG neurones

(n=4, 6). The effects of Ba^{2+} and linopirdine on synaptic transmission were also investigated. Trains of 20 stimuli at 5, 10, 20 and 50 Hz were applied to the pre-ganglionic nerve process. Ba^{2+} and linopirdine had no effect on the fraction of successful post-ganglionic action potentials discharged. These M channel antagonists have distinct actions on membrane properties and evoked firing patterns of rat ICG neurones, some of which change with postnatal development. The M channel appears to have little functional role in synaptic transmission in the ICG.

Adams DJ & Cuevas J (2004). In Basic and Clinical Neurocardiology, ed. Armour JA & Ardell JL, pp. 1-60. Oxford University Press, New York.

This work was supported by the BHF and BBSRC.

Where applicable, the authors confirm that the experiments described here conform with the Physiological Society ethical requirements.

PC153

Gamma oscillations in acute slices recorded in submerged versus interface conditions

C. Lu[1], E.C. Toescu[2] and M. Vreugdenhil[1]

[1]Neurophysiology, University of Birmingham, Birmingham, West Midlands, UK and [2]Physiology, University of Birmingham, Birmingham, West Midlands, UK

Gamma (30-80 Hz) oscillations in the brain are associated with learning and memory (Herrmann et al. 2004). In vitro, gamma oscillations are often recorded under interface conditions and oscillations lasts for hours. To study the cellular mechanisms of gamma oscillations, we established an in vitro model of kainate-induced gamma oscillations under submerged conditions. Here we characterize this model and compare it with gamma oscillations induced under interface conditions.

Hippocampal slices 300 μM thick were cut from the ventral mouse hippocampus and kept in submerged conditions. Kainate (250 nM) induced gamma oscillations in the CA3 area that quickly peaked but than reduced to a steady-state level.

Submerged kainate-induced gamma power and frequency was critically dependent on temperature with an optimum around 29°C, whereas 32-34°C is optimal for the interface recording. The peak power and frequency of the oscillation induced by kainate (100 nM) was 19.3±8.5 μV^2 (n=5, mean±SD) and 12.6±1.7 Hz at 24°C; 32.6±15 μV^2 and 24.5±2.5 Hz at 29°C; and 7.5±3.1 μV^2 and 8.5±1.3 Hz at 36°C.

To achieve submerged gamma, a relatively high (5-7 ml/min) perfusion rate was required, as submerged gamma is very small (2±0.8 μV^2, n=4) with a perfusion rate of 2-3 ml/min commonly used in the interface condition. Optimal oxygenation was critical for kainate-induced gamma oscillations in the submerged condition, which was achieved by optimising oxygen pressure of the aCSF and by adding fine glass fibres on the bottom of the recording chamber that allow perfusion from both sides.

Mapping of gamma oscillation in hippocampus indicated that, like under interface conditions, gamma oscillations were strongest in area CA3c. Peak gamma power increased with kainate concentration (25–1000 nM), but the steady state gamma power was maximal at 100 nM. The development in gamma oscillations (to reach peak) was faster in submerged recording (2 to 5 min) than in interface conditions (>30 min). The steady-state of gamma oscillations was short (20-50 min versus hours in interface conditions); the amplitude of gamma power was smaller (30.4±22.7 μV^2 versus 550.2±316 μV^2 in interface, n=5); and the washout was quicker (5-15 min versus > 30 min in interface recording). Repeated application of the same concentration of kainate (100 nM) caused 331±92% increase (n=6) in the gamma power.

These observations indicate that gamma oscillations can be reliably induced under submerged conditions. The fast development and quick washout of gamma oscillations allows for using repeated application of kainate. However, submerged gamma is vulnerable to conditions that affect the metabolic state of the cells in the network, which are better under interface conditions.

Herrmann CS, Munk MH & Engel AK (2004). Trends Cogn Sci 8, 347-355.

We thank the MRC for funding of this research. We thank J.G.R. Jefferys for a stimulating environment and the use of vital equipment.

Where applicable, the authors confirm that the experiments described here conform with the Physiological Society ethical requirements.

PC155

Localisation and role of Kv3.4 potassium channels in CA1 pyramidal neurones in rats

J.R. Maltas, L. Atkinson, V. Vakharia, J. Deuchars and N. Morris

University of Leeds, Leeds, UK

A recent study described upregulation of voltage gated Kv3.4 potassium channels in early and late stages of Alzheimer's disease (Angulo et al. 2004). However, little is known about their distibution and functional roles in central neurones. We therefore sought to determine the localisation of channels containing Kv3.4 subunits in the hippocampal formation. Using immunohistochemistry, we find that of the Kv3 subfamily (Kv3.1-4) only Kv3.4 subunits are expressed in CA1 and CA3 pyramidal cells and present both pre- and post-synaptically at presumptive Schaffer collateral synapses on CA1 pyramidal cells. To investigate the functional role of channels containing Kv3.4 subunits we performed whole-cell patch clamp recordings from CA1 pyramidal cells in 300 μm hippocampal brain slices obtained from 12 day old rats (data are presented as mean ± S.E.M., where n=number of cells). Voltage steps from -90 mV to +40 mV produced rapidly activating outward potassium currents with a large transient component in CA1 pyramidal cells. Application of the Kv3.4 subunit toxin blood depressing substance (BDS-II) at 50-100 nM significantly reduced the transient component of the outward current (peak current density reduced from 207 ± 36 to 72 ± 30 pA/pF; n=5; $P<0.05$ Student's T test) and shifted the $V_{1/2}$ from -15 ± 3 mV to -23 ± 2 mV (single Boltzmann function, n=5). We also have preliminary evidence that blocking Kv3.4 channel subunits increases action potential duration in CA1 pyramidal cells and alters the amplitude of evoked EPSCs. Our data suggest a role for channels containing Kv3.4 subunits in regulat-

ing intrinsic excitability and synaptic transmission in hippocampal neurones.

Angulo E et al. (2004). J Neurochem 91, 547-557.

Where applicable, the authors confirm that the experiments described here conform with the Physiological Society ethical requirements.

PC156

The action of the intravenous anaesthetic ketamine on ACh-evoked responses and synaptic transmission in rat intracardiac ganglia

A.A. Harper[1], K. Rimmer[1] and D.J. Adams[2]

[1]Molecular Physiology, University of Dundee, Dundee, UK and [2]School of Biomedical Sciences, University of Queensland, Brisbane, QLD, Australia

The dissociative intravenous anaesthetic, ketamine, has recently been shown to inhibit nicotinic acetylcholine receptor (nAChR)-mediated currents in dissociated neonatal rat intracardiac ganglion (ICG) neurones (Weber et al. 2005). This effect would be predicted to reduce the excitatory post synaptic potential amplitude and depress synaptic transmission in the ICG and would account for the action of ketamine on peripheral vagal transmission to the heart (Inoue & Konig, 1988).

We have investigated the actions of ketamine on postsynaptic responses to vagal nerve stimulation and exogenous ACh in adult rat ICG neurones. An isolated whole-mount preparation was used, comprising the right atrial ganglionic plexus and underlying myocardium. Intracellular recordings were made using sharp glass microelectrodes and the preparation was superfused with a bicarbonate buffered physiological salt solution maintained at 37°C.

The effects of ketamine on synaptic transmission were investigated by applying trains of 20 stimuli at 5-100 Hz to the preganglionic nerve trunk. Ketamine attenuated postsynaptic action potential firing during each train in a concentration-dependent manner. This inhibition was more marked at higher frequencies (see Fig. 1). Attenuation of synaptic transmission in ICG was apparent at clinically relevant concentrations (10 μM), the fraction of suprathreshold responses being reduced to 0.62 (± 0.14 SD, n=3) of control values at 10 Hz by 100 μM ketamine.

Focal application of ACh (100 μM, ≤10 ms) to ICG neurons evoked membrane depolarization and action potential discharge. This excitatory response was reversibly inhibited in a concentration-dependent manner by ketamine. Superfusion of ketamine (100 μM) reduced the excitatory response to exogenous ACh to 0.35 (± 0.10, n=3) of control depolarizing responses, but had no effect on the excitatory responses evoked by focal application of GABA (see Fischer et al. 2005). Taken together, ketamine inhibits ACh-induced responses and synaptic transmission in rat ICG and therefore attenuates the bradycardia observed in response to vagal stimulation in the mammalian heart.

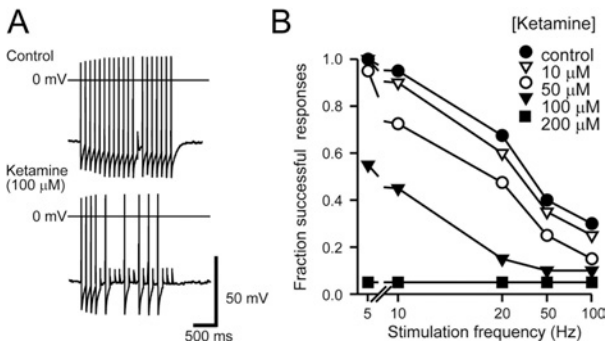

Figure 1. Attenuation of postsynaptic events evoked by trains of nerve stimuli in the presence of ketamine. A, responses to a train of 20 stimuli at 10Hz delivered to the preganglionic nerve trunk in control conditions and during superfusion of ketamine (100 μM). B, depression of action potential firing recorded during repetitive stimuli with increasing concentrations of ketamine. The ratio of the number of suprathreshold responses to the number of stimuli was used to give an index of the frequency dependence of synaptic transmission.

Fischer H, Harper AA, Anderson CR & Adams DJ (2005). J Physiol 564, 465-474.

Inoue K & Konig LA (1988). Br J Anaesth 61, 456-461.

Weber M, Motin L, Gaul S, Beker F, Fink RH & Adams DJ (2005). Br J Pharmacol 144, 98-107.

A.A.H. thanks the British Heart Foundation for support. K.R. is a BBSRC Student.

Where applicable, the authors confirm that the experiments described here conform with the Physiological Society ethical requirements.

PC157

Magnesium block of NMDA receptors in dopaminergic neurons of neonatal rat substantia nigra pars compacta

Z. Huang and A.J. Gibb

Pharmacology, University College London, London, UK

Activation of NMDA receptors in substantia nigra pars compacta (SNc) dopaminergic neurones induces a voltage-dependent burst firing (Johnson et al. 1992) that regulates dopamine release in the striatum. The voltage dependence of magnesium block of NMDA receptors is a critical determinant of their normal physiological role. In SNc, NMDA receptors may be triheteromers of NR1, NR2B and NR2D subunits (Jones & Gibb, 2005) and thus could have an unusual voltage dependence. We have used patch-clamp whole-cell recording methods to quantify magnesium block of NMDA receptors in 300 μm thick coronal slices of SNc from 7 day old rats.

Responses to 0.01 mM NMDA and 0.01 mM glycine in the presence of TTX (100 nM) with 3mM ATP and 1mM GTP in the pipette solution were recorded and the voltage dependence of the net whole-cell NMDA current evoked during voltage ramps (-100 mV to +40 mV of 2 s duration) in the absence of magnesium, and in the presence of 0.1 mM or 1.0 mM

magnesium quantified using a model that included the possibility of magnesium block of the NMDAR channel from both outside and inside as well as binding of magnesium to a voltage-independent potentiation site on the extracellular site of NR2B subunit-containing receptors (Paoletti et al. 1997). Of the tested neurons 85% showed a hyperpolarisation-activated slow inward current (Ih current) characteristic of dopaminergic cells and in these cells at -60 mV, 0.1 mM magnesium blocked the NMDA current by 35.3–72.5% while 1.0 mM magnesium blocked the NMDA current by 83.7–93.5% (n = 6 cells). Using the current-voltage relation from these cells we estimate the fraction (delta) of the membrane field sensed by magnesium at it's binding site to be 0.54 and the dissociation equilibrium constant for binding at 0 mV (Kb(0mV)) to be 1.3 mM. These results suggest that the voltagedependence of magnesium block of NMDA receptors in SNc cells is more similar to that observed for NR2C or NR2D subunit-containing NMDA receptors than for NR2A or NR2B receptors.

Johnson SW, Seutin V & North RA (1992). Science 258, 665-667.

Jones S & Gibb AJ (2005). J Physiol 569, 209-221.

Paoletti P, Neyton J & Ascher P (1997). Neuron 15, 1109-1120.

Supported by the Wellcome Trust. Z.H. is funded by an Overseas Research Studentship.

Where applicable, the authors confirm that the experiments described here conform with the Physiological Society ethical requirements.

PC158

The effect of '*in vitro* ageing' on mitochondrial Ca^{2+} regulation and neuronal vulnerability

M.S. Chitolie and E.C. Toescu

Dept. of Physiology, University of Birmingham, Birmingham, UK

Glutamate (Glu) stimulation of neuronal cells induces cytosolic Ca^{2+} ($[Ca^{2+}]_c$) increases, which can reach the threshold for activation of the mitochondrial Ca^{2+} uniporter [1]. In this study we used an *in vitro* model of neuronal ageing [2] which consists of long-term primary cultures of cerebellar granule neurones obtained from Wistar rat pups (P5-8). The aim of the present study was to investigate the effect of such '*in vitro* ageing' on the relationship between the Glu-evoked $[Ca^{2+}]_c$ and mitochondrial Ca^{2+} ($[Ca^{2+}]_m$) load.

Neurones loaded with Fura-2-AM (2.5μM) were stimulated with Glu (2-200μM in 0Mg/Gly) followed after a wash period, by the protonophore CCCP (10μM) to unload the mitochondria. The parameters investigated were the amplitude of the Glu-evoked Ca^{2+} signal and the amplitude of the CCCP-induced Ca^{2+} signal.

We show that with time in culture there is an increase in the size of the Glu-evoked Ca^{2+} signal. In young neurones (days *in vitro* (DIV) 7-15), 20μM Glu induced a 2.25-fold increase ±0.32 (S.E.M., n=5 experiments, each with >20 neurones) in the Ca^{2+} signal, whereas in the older neurones (DIV 21-50) the increase was significantly larger (4.28-fold increase ±0.08 S.E.M., n=4; t test, $p<0.001$). By measuring the amplitude of the CCCP-evoked Ca^{2+} signals post-Glu challenge, we estimated the size of the $[Ca^{2+}]_m$ load. We found that the larger increases in $[Ca^{2+}]_c$ signals in the older neurones were associated with significantly larger $[Ca^{2+}]_m$ loads (in the older neurones: 2.72-fold increase ±0.44 S.E.M., n=4 versus 1.76-fold increase ±0.09 S.E.M., n=5, in the young neurones; t test, $p<0.02$). The two parameters, Glu-evoked Ca^{2+} signal and CCCP-evoked Ca^{2+} signals, were correlated indicating that the size of the cytosolic Ca^{2+} challenge is one of the most important controllers of the $[Ca^{2+}]_m$ load. This is important, since previous work has shown that the mitochondria in aged neurones are chronically depolarised [2,3] and thus potentially less able to accumulate Ca^{2+} due to a decreased electrochemical gradient.

Finally, we also investigated whether the changes in Glu-evoked Ca^{2+} responses were associated with changes in vulnerability. Neurones at various DIVs were incubated in Glu for 2h and the amount of neuronal death was dynamically quantified using propidium iodide (50μg/ml) fluorescence. With this method, we show that with increasing age *in vitro*, there is a clear-cut increase in neuronal vulnerability.

In conclusion we report that *in vitro* ageing increases the amplitude of the Glu-evoked Ca^{2+} signals and increases significantly the $[Ca^{2+}]_m$ load. Also, older neurones become more vulnerable to the effects of Glu stimulation and are more susceptible to Glu excitotoxicity. This suggests that the $[Ca^{2+}]_m$ load, driven by the $[Ca^{2+}]_c$ signal is a key component of the increased vulnerability of aged neurones to Glu.

Brocard JB, Tassetto M & Reynolds IJ (2001). J Physiol **531**, 793-805.

Xiong J, Verkhratsky A & Toescu EC (2002). J Neurosci **22**, 10761-10771.

Xiong J et al. (2004). Neurobiol Aging **25**, 349-359.

Where applicable, the authors confirm that the experiments described here conform with the Physiological Society ethical requirements.

PC159

Absence of P2Y receptor modulation of NMDA currents in neonatal rat striatum

E. Coppi[2], F. Pedata[2] and A.J. Gibb[1]

[1]Pharmacology, University College London, London, UK and [2]Pharmacology, University of Florence, Florence, Italy

Metabotrophic P2Y ATP receptors are widely distributed throughout the brain (Ralevic & Burnstock, 1998) and P2Y1 receptor protein is found in the striatum of both humans and rats (Franke et al. 2003; Scheibler et al. 2004). Via activation of protein kinase C and increases in intracellular calcium, P2Y1 receptors have the potential to influence a variety of voltage-dependent and neurotransmitter-activated ion channels during development and in the adult brain. Here we investigated the possibility that P2Y receptor activation may modulate NMDA receptor responses in striatal slices from 7 day old rats.

Two minute whole-cell responses to 0.01 mM NMDA and 0.01 mM glycine in the presence of TTX (100 nM) were recorded with ATP (2 mM) and GTP (0.5 mM) in the pipette solution in 17 neurones. Steady-state control responses to NMDA (133 ± 27.2 pA) were recorded followed by a 5 min application of the P2Y agonist, 2-methyl-thio-ADP (2-Me-S-ADP, 250 nM). Following this, NMDA was applied again for a further 2 min in the presence of 2-Me-S-ADP and the mean NMDA current recorded (121 ± 24.5 pA). In control experiments, NMDA was applied twice at 5 min intervals in the absence of 2-Me-S-ADP and the second response was 90.1 ± 4.7% of the first response. In the presence of the P2Y agonist, the NMDA response was 89.3 ± 6.1% of the control current and we therefore conclude that there is no significant effect (n = 17 cells, paired t-test, P>0.05) of P2Y receptors on NMDA responses under these conditions.

Ralevic V & Burnstock G (1998). Pharmacol Rev 50, 413-492.

Franke H, Kittner H, Grosche J & Illes P (2003). Psychopharmacology 167, 187–194.

Scheibler et al. (2004). Br J Pharmacol 143, 119–131.

Supported by the Wellcome Trust. E.C. is funded by a University of Florence Postgraduate Fellowship.

Where applicable, the authors confirm that the experiments described here conform with the Physiological Society ethical requirements.

PC160

The ionic stoichiometry of the glutamate transporter GLAST in salamander retinal glia

S. Gylterud Owe[1], P. Marcaggi[2] and D. Attwell[2]

[1]Dept. Anatomy, University of Oslo, Oslo, Norway and [2]Dept. Physiology, University College London, London, UK

High affinity glutamate receptors may be activated by the baseline extracellular glutamate concentration, $[Glu]_o$. The most abundant glutamate transporter, GLT-1, could lower $[Glu]_o$ to ~2nM, based on its ionic stoichiometry and the concentrations of its driving ions, Na^+, K^+ and H^+, but measurements using microdialysis give a value of ~1μM (Cavelier et al. 2005).

If other glutamate transporters had a different stoichiometry, the minimum glutamate concentration could be higher, for example if those transporters were driven by the co-transport of 2 Na^+ (rather than of 3 Na^+ as for GLT-1). Here we investigated the ionic stoichiometry of the glutamate transporter GLAST, which is highly expressed in the retina and cerebellum, and is present throughout the brain early in development when expression of GLT-1 is low.

Müller cells from salamander retina were dissociated and whole-cell patch-clamped to monitor glutamate transport as a membrane current (Brew & Attwell, 1987). These cells express homologues of the mammalian transporters GLAST, GLT-1 and EAAT5 (Eliasof et al. 1997), but the low sensitivity of their transport current to dihydrokainate and the absence of a large transporter anion conductance imply that GLAST is the only transporter that generates a significant current. The internal and external solutions lacked Cl^- ions to abolish currents generated by the transporter's anion conductance. With glutamate, Na^+, K^+ and H^+ present on both sides of the membrane the direction of transport at different voltages was assessed by blocking transporter action with TBOA (cf. Levy et al. 1998). The reversal potential for the TBOA-blocked current is determined by the transporter stoichiometry.

We measured the transporter reversal potential using a standard pair of intra- and extracellular solutions, and then with the external $[Na^+]$ reduced by 1/3, the external [glutamate] increased 5-fold, the external $[H^+]$ increased 2.5-fold, or the external $[K^+]$ decreased 2.5-fold. For all these manipulations the measured change of reversal potential was within a few mV of (not significantly different from) that predicted for a stoichiometry in which each glutamate anion is co-transported with 3 Na^+ and 1 H^+ while 1 K^+ is counter-transported, as previously found for GLT-1 and EAAC1 (Zerangue & Kavanaugh, 1996; Levy et al. 1998), and was significantly different to the prediction for the case of 2 Na^+ being transported.

The demonstration that the stoichiometry of GLAST is the same as that for GLT-1 suggests that the minimum extracellular glutamate concentration should be similar during development and in the adult brain. A less powerful accumulation of glutamate by GLAST than by GLT-1 cannot be used to explain the high glutamate concentration measured by microdialysis.

Brew H & Attwell D (1987). Nature 327, 707-709.

Cavelier P, Hamann M, Rossi D, Mobbs P & Attwell D (2005). Prog Biophys Molec Biol 87, 3-16.

Eliasof S, Arriza JL, Leighton BH, Kavanaugh MP & Amara SG (1997). J Neurosci 18, 698-712.

Levy LM, Warr O & Attwell D (1998). J Neurosci 18, 9620-9628.

Zerangue N & Kavanaugh MP (1996). Nature 383, 634-637.

Supported by the Wellcome Trust and the Norwegian Research Council.

Where applicable, the authors confirm that the experiments described here conform with the Physiological Society ethical requirements.

PC161

A developmental change in functional NR2B subunit expression at glutamatergic synapses in substantia nigra *pars compacta* dopaminergic neurones

S.L. Brothwell[1], J.L. Barber[1], A.J. Gibb[2] and S. Jones[1]

[1]Department of Physiology, Development and Neuroscience, University of Cambridge, Cambridge, UK and [2]Department of Pharmacology, University College London, London, UK

NMDA glutamate receptors (NMDARs) on substantia nigra *pars compacta* (SNc) dopaminergic (DA) neurones influence action potential firing patterns, forms of synaptic plasticity and may contribute to excitotoxic neurodegeneration of DA neurones in Parkinson's disease. NMDARs are hetero-oligomers and their functional diversity is mainly determined by NR2 (A-D) subunits. In cortical areas, NR2 subunit expression changes during critical periods of development, with NR2A subunits replacing or joining NR2B subunits at excitatory synapses. The subunit composition of functional synaptic NMDARs in midbrain DA neurones during postnatal development is not known. We have

used whole-cell patch-clamp recording methods in midbrain slices (300 μm) to determine the contribution of NR2B subunits to NMDAR-mediated evoked excitatory postsynaptic currents (EPSCs) in DA neurones from rats aged postnatal day (P)6 to P22.

NMDAR-mediated EPSCs, isolated pharmacologically, were observed at all ages tested (P6-P22). NMDAR-mediated EPSCs were inhibited by D-AP5 (50 μM) and showed the expected voltage-dependent sensitivity to Mg^{2+} ions. In order to determine whether NR2B subunits form NMDARs in SNc DA neurones, we used the non-competitive antagonist ifenprodil (3-10 μM) which preferentially inhibits NR2B subunits. NMDARs in SNc DA neurones were sensitive to 3-10 μM ifenprodil at all ages tested. There was a significant decrease in the inhibitory effect of ifenprodil (10 μM) between the first and second weeks of postnatal development (P6-P8: 72.0 ± 1.5%; n = 5; P13-15: 57.9 ± 3.8% inhibition; n=13; $p<0.005$). No further significant change in ifenprodil sensitivity was observed between the second and third weeks of postnatal development (P20-22: 51.8 ± 7.2% inhibition; n=9; $p = 0.5$). These data suggest that NR2B subunits form functional NMDARs at excitatory synapses in SNc DA neurones, and contribute to NMDAR-mediated EPSCs throughout postnatal development. However, the contribution of NR2B subunits decreases early in postnatal development, and an ifenprodil-insensitive component remains.

Where applicable, the authors confirm that the experiments described here conform with the Physiological Society ethical requirements.

PC162

Matching energy supply and expenditure to computation in the cerebellum

C. Howarth, C.M. Peppiatt, P. Mobbs and D. Attwell

Physiology, UCL, London, UK

The processing power of computational devices is limited by their energy supply (Laughlin & Sejnowski, 2003). The division of brain energy use between neuronal resting potentials, synaptic potentials and action potentials is broadly understood (Attwell & Laughlin, 2001), but in general it is unknown how the energetic resources available to the brain are allotted to carry out different parts of a neural computation.

We analysed the relationship between energy expenditure and information processing for the cerebellar cortex, a brain area for which the cellular properties and computations performed have been well studied. Most signalling-related energy in the brain is expended on pumping of Na^+ ions out of the cell (Siesjo, 1978; Attwell & Laughlin, 2001). We estimated the signalling energy expended in the rat cerebellum by using published anatomical and electrophysiological data on the properties of the different cerebellar cells to calculate the Na^+ influx producing excitatory synaptic currents and action potentials, the Na^+ influx occurring at the resting potential, and the Ca^{2+} entry driving excitatory and inhibitory transmitter release (Attwell & Laughlin, 2001). As in previous work (Attwell & Laughlin, 2001), these fluxes were converted into values for ATP consumption. We predict the total ATP consumption on signalling (summed over all cell types) to be ~27μmol/g/min, slightly greater than the 20μmol/g/min measured in anaesthetized albino rats (Sokoloff et al. 1977).

We estimate that each Purkinje cell uses $1.6x10^{10}$ ATP/s, whereas the much smaller granule cell uses approximately $3x10^8$ ATP/s. However, the much larger number of granule cells results in them consuming the great majority of the cerebellar cortical energy. Thus, most energy goes on granule cells re-mapping the sensory and motor command input arriving on the mossy fibres into a sparsely coded representation used by the Purkinje cells to retrieve motor output patterns.

Spatially, signalling energy use was predicted to be split between the granular, Purkinje cell soma and molecular layers in the ratio 30%: 2%: 68%. Comparing the capillary area available for O_2 and glucose supply to the different cerebellar cortical layers suggests that the blood supply to these layers is only approximately matched to the computations carried out in each layer.

Our results, together with the calculations of Brunel et al. (2004), suggest that for each Purkinje cell (and associated other neurons and glia) approximately 10^{11} molecules of ATP/s are used per 5kb of retrievable motor information, corresponding to an energy storage cost of 1mW/GB.

Attwell D & Laughlin SB (2001). *J Cereb Blood Flow Metab* **21,** 1133-45.

Brunel N, Hakim V, Isope P, Nadal JP & Barbour B (2004). *Neuron* **43,** 745-757.

Laughlin SB & Sejnowski TJ (2003). *Science* **301,** 1870-1874.

Siesjo B (1978). Brain Energy Metabolism. New York, Wiley.

Sokoloff L, Reivich M, Kennedy C, Des Rosiers MH, Patlak CS, Pettigrew KD *et al.* (1977). *J Neurochem* **28,** 897-916.

Supported by the Wellcome Trust, EU and a Wolfson-Royal Society Award. C.H. is in the 4 year PhD programme in Neuroscience at UCL.

Where applicable, the authors confirm that the experiments described here conform with the Physiological Society ethical requirements.

PC163

Different subtypes of NG2-positive glia in the white matter of rat cerebellar slices

R.T. Karadottir and D. Attwell

Department of Physiology, University College London, London, UK

For normal function of the nervous system, oligodendrocytes are needed to speed the propagation of the action potential. In diseases like cerebral palsy, spinal cord injury and multiple sclerosis, oligodendrocytes get damaged and the action potential is slowed or abolished. Replacement of damaged oligodendrocytes, either by endogenous or perhaps transplanted cells, is essential to restore normal function.

In the adult brain more than 5% of the cells are glia that express the proteoglycan NG2 (Dawson et al. 2003). The function of these cells is poorly understood. They are generally thought to be oligodendrocyte precursor cells, which might replace myelinating oligodendrocytes that become damaged. However, they have recently been suggested to be either multipotent stem cells able to gener-

ate both GABAergic neurons and oligodendrocytes (Aguirre et al. 2004), or a new type of glia called synantocytes which contact the nodes of Ranvier (Butt et al. 1999). Because of this controversy over their function, we have examined the origins of these cells with immunohistochemistry and studied their electrical properties by whole-cell clamping. Dye filling from the whole-cell pipette allowed us to study the cells' morphology and recover the recorded cell for antibody labelling (Káradóttir et al. 2005).
In the white matter of cerebellar slices at postnatal day 7, most NG2 glia are part of the oligodendrocyte lineage: 93% of 106 cells which labelled with antibody to NG2 were also labelled by antibody against the oligodendrocyte transcription factor Olig2. However, these NG2/Olig2 positive cells could be divided into two subtypes with distinct electrophysiological properties. One subtype showed a TTX-sensitive sodium current, followed by a slowly developing outward rectifying current presumably mediated by voltage-gated potassium channels, in response to depolarizing voltage steps. The other subtype did not show these voltage-gated currents. Interestingly, although both subtypes responded to superfused GABA and glutamate, only the subtype expressing the voltage-gated channels also received action potential driven synaptic input, both GABA-ergic and glutamatergic, which was TTX sensitive.
These data suggest that two subtypes of oligodendrocyte precursor exist, with distinct electrophysiological characteristics, contrary to current assumptions. Only the subtype expressing voltage-gated channels senses its neuronal environment by receiving synaptic input from passing axons. Conceivably one of these subtypes may be destined to myelinate axons immediately, and the other may become the 'adult precursors' which can differentiate into myelinating oligodendrocytes after pathological conditions.

Aguirre AA, Chittajallu R, Belachew S & Gallo V (2004). J Cell Biol 165, 575-589.

Butt AM, Duncan A, Hornby MF, Kirvell SL, Hunter A, Levine JM & Berry M (1999). Glia 26, 84-91.

Dawson MR, Polito A, Levine JM & Reynolds R (2003). Mol Cell Neurosci 24, 476-488.

Káradóttir R, Cavelier P, Bergersen L & Attwell D (2005). Nature 438, 1162-1166.

Supported by the Wellcome Trust.

Where applicable, the authors confirm that the experiments described here conform with the Physiological Society ethical requirements.

PC164

Functional significance of plasma membrane Ca^{2+} ATPase splice variant 2a at excitatory pre-synaptic terminals in the rat hippocampal CA3 region

T. Jensen[1], A. Filoteo[2] and R.M. Empson[1]

[1]School of Biological Sciences, Royal Holloway, University of London, Egham, Surrey, UK and [2]The Program in Molecular Neuroscience, Department of Biochemistry and Molecular Biology, Mayo Graduate School, Mayo Clinic, Rochester, MN, USA

Plasma membrane calcium ATPases (PMCAs) use energy derived from ATP to drive Ca^{2+} from the cytosol into the extracellular fluid. PMCAs act as a highly efficient primary route for removing intracellular Ca^{2+} ($[Ca^{2+}]_i$) at sub-micromolar concentrations (Thayer et al. 2002). As the product of 4 genes (PMCA1-4) PMCAs are alternatively spliced to produce 20 identified splice variants. It is believed that alternative splicing may localise specific PMCA splice variants to synapses and that these splice variants may regulate synaptic transmission by controlling $[Ca^{2+}]_i$ at these sites (Strehler & Zacharias, 2001).
Here we investigated the synaptic localisation of the neurone-specific PMCA2 splice variant PMCA2a and examined its function in the regulation of excitatory synaptic transmission in the CA3 region of organotypic hippocampal slices.
Organotypic hippocampal slices were prepared from 7 day old Wistar rat pups (Stoppini et al. 1991) and were maintained for 10-14 days *in vitro* before they were used for electrophysiology or immunohistochemistry. Confocal fluorescence microscopy was carried out as previously described (Buckby et al. 2006) and co-localisation was quantified using Bio-Rad Lasersharp software. Whole-cell patch clamp recordings of evoked excitatory post-synaptic currents (EPSCs) from CA3 pyramidal neurones held at -70mV were carried out in the presence of 10μM bicuculline, 5μM CGP52432 and 0.5μM NBQX using an Axoclamp 2B patch clamp amplifier in voltage clamp mode.
Using PMCA splice-variant specific antibodies we show that the PMCA2 splice variant PMCA2a is enriched in forebrain synaptosomes and co-localises with the pre-synaptic marker synaptophysin but not the post-synaptic marker PSD-95. Furthermore, PMCA2a co-localised at pre-synaptic terminals immunopositive for the excitatory pre-synaptic terminal marker VGLUT1 but not the inhibitory pre-synaptic terminal marker GAD-65 indicating that PMCA2a is localised specifically to excitatory pre-synaptic terminals.
Whole cell patch clamp recordings showed that treatment of slices with the specific PMCA inhibitor carboxyeosin (CE) significantly enhanced paired pulse facilitation (PPF) lengthening the time course of PPF. For example CE treatment enhanced PPF with a 50ms inter-stimulus interval from a paired pulse ratio (EPSC2/EPSC1) of 2.13±0.19 (mean ± SEM) to 2.98±0.16 in 10μM CE-treated slices ($n=6$, $p<0.01$ paired t test) without affecting the mean amplitude of the 1st EPSC ($p=0.78$, $n=6$ paired t-test) indicating a pre-synaptic effect of PMCA inhibition.
These results show that PMCA2a splice variants localise to excitatory pre-synaptic terminals and regulate excitatory synaptic transmission presumably by their role in controlling residual $[Ca^{2+}]_i$.

Stoppini L et al. (1991). J Neurosci Methods 37, 173-182.

Strehler EE & Zacharias DA(2001). Physiol Rev 81, 21-50.

Thayer SA (2002). Front Biosci 7, d1255-d1279.

Buckby LE et al. (2006). Molecular and Cellular Neuroscience (in press).

This work was funded by the Epilepsy Research Foundation, UK.

Where applicable, the authors confirm that the experiments described here conform with the Physiological Society ethical requirements.

PC165

Glutamine transporter currents recorded from the rat calyx of Held synapse

B. Billups

Cell Physiology and Pharmacology, University of Leicester, Leicester, UK

The principle route for recycling glutamate at central excitatory synapses is thought to be via the glutamate-glutamine cycle. This involves the uptake of glutamate into glial cells, conversion to glutamine by the enzyme glutamine synthase and subsequent transport out of the glial cells by the system N transport. The cycle is completed by the transport of glutamine into the presynaptic terminal via the system A transporters and conversion into glutamate by phosphate-activated glutaminase (Chaudhry et al. 2002a). Although currents generated by the electrogenic system A transporters have been demonstrated in expression systems and some postsynaptic cells (Chaudhry et al. 2002b), direct electrical recording of this transporter's activity from presynaptic terminals has not been shown. Using patch-clamp recordings from rat brainstem slices I have been able to demonstrate the presence of electrogenic system A transporter currents in both postsynaptic cells and presynaptic terminals at the calyx of Held synapse.

Brainstem slices were prepared from Lister Hooded rats (P9 to 12). Postsynaptic medial nucleus of the trapezoid body (MNTB) cells or presynaptic calyx of Held terminals were whole-cell voltage-clamped and all recordings performed at 35-37°C. All data are represented as mean ± SEM.

Puff application of glutamine (10 mM for 1 s) elicited an inward current in postsynaptic MNTB neurones held at –70mV. This current was not blocked by inhibitors of ionotropic glutamate, GABA or glycine receptors (22.1 ± 1.7 pA in control, 21.0 ± 2.3 pA in blockers, n=6, P=0.71, 2-tailed t test), but was inhibited by the system A-specific analogue 2-(methylamino)isobutyrate (10 mM MeAIB; 3.3 ± 0.8 pA, n=6, P<0.01, 2-tailed t test). Moreover, the current did not reverse at depolarized membrane potentials, consistent with properties of system A transport (Chaudhry et al. 2002b). Similar currents were also recorded from the calyx of Held presynaptic terminal, where puff application of glutamine evoked a current of 12.1 ± 2.6 pA (n=5). This current was inhibited by 54 ± 6% upon application of 10 mM MeAIB (n=5, P=0.01, 2-tailed paired t test), indicating a significant system A transporter component.

These data show for the first time the presence of system A transporter currents in presynaptic terminals *in situ*, demonstrating their potential importance in glutamate recycling. It will also allow the regulation of this transporter to be studied in a synaptic preparation and permit investigations into the role it plays in supplying the glutamate needed to sustain neurotransmission.

Chaudhry FA, Reimer RJ & Edwards RH (2002a). J Cell Biol 157, 349-55.

Chaudhry FA, Schmitz D, Reimer RJ, Larsson P, Gray AT, Nicoll R, Kavanaugh M & Edwards RH (2002b). J Neurosci 22, 62-72.

Supported by The Royal Society and The Wellcome Trust.

Where applicable, the authors confirm that the experiments described here conform with the Physiological Society ethical requirements.

PC166

Quantal transmitter release from axonal varicosities and cell bodies of noradrenergic neurones in rat brainstem slice culture detected by amperometry

Z. Chiti and A.G. Teschemacher

Department of Pharmacology, Bristol Heart Institute, School of Medical Sciences, University of Bristol, Bristol, UK

Central noradrenaline (NA) release impacts on many vital physiological functions, for example blood pressure control (Duale et al. 2005). In order to understand the mechanisms regulating NA secretion in the brain, we need to characterise vesicle fusion events in central noradrenergic (NAergic) neurones. In addition, it was previously uncertain whether NA release occurs only from varicosities or also from soma and dendrites, although the distribution of release sites is the key determinant for the impact of secreted NA in the brain. Indeed, while release from axonal terminals will activate receptors in target areas, somato-dendritic release may result in autoinhibition of NAergic neurones and affect adjacent interneurones within NAergic nuclei.

Microamperometry was used to directly measure release from NAergic neurones expressing enhanced green fluorescent protein in organotypic brainstem slice cultures (Teschemacher, 2004; Teschemacher et al. 2005). Oxidation spikes were registered at a driving voltage of +800 mV using stiff carbon fibre microelectrodes (active surface tip diameter ~5 μm) which were placed onto green fluorescent somata or axonal varicosities of NAergic neurones.

Our data suggest NA release from two major populations of secretory vesicles. The main population of events measures median (±s.e.m.) values for amperometric charge: 0.04 ±0.004 pCoulomb; amplitude: 8.3 ±0.5 pA; and half time: 3.2 ±0.14 ms (n=16). These properties are not significantly different between somato-dendritic and axonal release sites. Spike frequencies vary widely between individual release sites but, again, are not significantly different between the somato-dendritic compartment and axons. Assuming that intravesicular NA concentration in central neurones is comparable to that proposed for adrenal chromaffin cells, these results suggest that the majority of NA-secreting vesicles in the brain are small with diameters ranging around 75 nm, consistent with electron microscopy data (Bloom & Aghajanian, 1968; Travis & Wightman, 1998). In addition, at about 25% of release sites, we also registered large release events consistent with vesicle diameters of 300-400 nm. While these events represented only about 5% of the total spike population, due to their high charge, they contributed about 25% to the total NA release registered at these sites. The majority (~80%) of the large events was registered at axonal release sites.

We conclude that exocytosis occurs from both, axonal varicosities and the somato-dendritic compartments, of central NAergic neurones. Our data further suggest that some axonal release sites may, in addition, utilise very large vesicles which appear comparable to adrenal chromaffin cell granules.

Bloom FE & Aghajanian GK (1968). J Pharmacol Exp Ther 159, 261-273.

Duale H, Teschemacher AG, Waki H, Kasparov S & Paton JF (2005). J Physiol 567P, PC39.

Teschemacher AG (2004). J Physiol 555P, PC40.

Teschemacher AG, Wang S, Lonergan T, Duale H, Waki H, Paton JF & Kasparov S (2005). Exp Physiol 90, 61-69.

Travis ER & Wightman RM (1998). Annu Rev Biophys Biomol Struct 27, 77-103.

Supported by the British Heart Foundation, the Royal Society, and the Wellcome Trust (VIP award to Z.C.).

Where applicable, the authors confirm that the experiments described here conform with the Physiological Society ethical requirements.

PC167

GABAergic IPSCs in the tuberomamillary nucleus and in the perifornical area of the hypothalamus are insensitive to prolongation by the general anaesthetic propofol in the N265M knock-in mouse

A. Zecharia[1], M. Schumacher[1], R. Jurd[2], U. Rudolph[2], M. Maze[1] and N.P. Franks[1]

[1]Biophysics Section, Imperial College London, London, UK and [2]Institute of Pharmacology and Toxicology, University of Zurich, Zurich, Switzerland

The mechanisms by which general anaesthetics produce a loss of consciousness are unknown. However, the EEG suggests similarities between this state and that of non-REM sleep. We are investigating the hypothesis that these drugs interact with endogenous sleep pathways. In particular, a GABAergic nucleus in the hypothalamus called the ventrolateral preoptic area (VLPO) is activated specifically during sleep [1], and increases its firing in proportion to sleep depth. Moreover, lesions of this nucleus produce insomnia. These neurons are believed to cause sleep through the inhibition of wake-active nuclei [2], including the histaminergic tuberomamillary nucleus (TMN) and the orexinergic neurons of the perifornical area (PeF). The GABAergic nature of the VLPO is critical to this hypothesis of anaesthetic action because these drugs potentiate the $GABA_A$ receptor *in vitro*. Furthermore, mice with a point-mutation (N265M) in the β_3 subunit of this receptor are markedly less sensitive to the hypnotic action of propofol and etomidate, but retain sensitivity to the steroid anaesthetic alphaxalone [3]. Previous work from this laboratory suggests that the TMN is an important neuronal target for general anaesthetics [4]. The TMN receives additional excitation from the orexinergic neurons of the PeF during the waking state [5] and c-fos data (unpublished) indicates that these neurons are inhibited by GABAergic anaesthetics.

We are using hypothalamic coronal slices to compare the ability of propofol (1.5 μM) and alphaxalone (2 μM) to prolong the decay of whole-cell GABAergic IPSCs in both the TMN and PeF of adult male wild-type and N265M knock-in 129/SvJ mice. The decay time constant was calculated as the IPSC integral divided by its peak. All recordings were made at room temperature. Under control conditions, the IPSC decay time was not significantly different in wild-type compared to knock-in animals.

In the wild-type TMN, IPSCs were prolonged by both propofol (141 ± 24%, mean ± s.e.m. shown for all data; n=7) and alphaxalone (237 ± 25%; n=5). Strikingly, IPSCs in the TMN of the N265M knock-in mouse were found to be insensitive ($P<0.001$, 2-tailed, unpaired Student's t test) to prolongation by propofol (23 ± 8%; n=9). However, again mirroring *in vivo* findings, the ability of alphaxalone to prolong the IPSC decay time (218 ± 48%; n=4) was retained in the knock-in mouse.

Similar data were obtained for the orexinergic neurons of the PeF: these neurons were insensitive ($P<0.01$) to propofol (10 ± 10%; n=4) in the knock-in mouse compared to wild-type (116 ± 25%; n=5) whereas responses to alphaxalone did not differ.

These findings are consistent with the hypothesis that enhancement of GABAergic input into hypothalamic wake-active nuclei is an integral part of propofol's mechanism of action *in vivo*.

Sherin JE *et al.* (1996). *Science* **271**, 216-219.

Steininger TL *et al.* (2001). *J Comp Neurol* **429**, 638-653.

Jurd R *et al.* (2003). *Faseb J* **17** 250-2.

Nelson LE *et al* (2002). *Nature Neurosci* **5** 979-984.

Eriksson KS *et al.* (2001). *J Neurosci* **21** 9273-9279.

Where applicable, the authors confirm that the experiments described here conform with the Physiological Society ethical requirements.

PC168

Cell target specific presynaptic actions of kainate receptors at individual mossy fibre synapses

R. Scott, D.M. Kullmann and D.A. Rusakov

UCL Institute of Neurology, London, UK

Hippocampal mossy fibres form distinct synapses on principal cells and interneurons. These synapses exhibit distinct forms of use-dependent plasticity, both short- and long-term. The mechanisms underlying this heterogeneity remain poorly understood. An important role in synaptic facilitation has been attributed to presynaptic kainate receptors, which have also been implicated in the initiation and maintenance of epileptiform activity. We have therefore examined the role of presynaptic kainate receptors at distinct presynaptic structures in rat mossy fibres.

We applied two-photon microscopy to address Ca^{2+} dynamics in individual mossy fibre boutons (MFBs), which were traced up to 1.5 mm from granule cell somata held in whole-cell mode. In giant MFBs forming synapses on CA3 pyramidal cells, blockade of kainate receptors with 25 μM NBQX increased the amplitude of evoked presynaptic Ca^{2+} transients following an action potential generated in a single cell by 36 ± 14% ($p < 0.04$, $n = 7$). Blocking kainate receptors also reduced short-term facilitation of presynaptic Ca^{2+} transients following repetitive spikes (paired-pulse ratio decreased by 52 ± 11%, $p < 0.005$). Blocking kainate receptors also abolished the contribution of Ca^{2+} stores to the evoked presynaptic Ca^{2+} signal (ryanodine decreased the $\Delta F/F$ Ca^{2+} signal under control conditions by 14 ± 3%, $n = 10$, but only by 3 ± 8%, $n = 8$, after application of NBQX). In contrast, in en-passant MFBs and in collateral axonal branches, both of which are presynaptic to interneurons, blockade of kainate receptors had no detectable effect on presynaptic Ca^{2+} signalling ($n = 7$ main axon boutons and $n = 8$ collateral branches). Consistent with this finding, the contribution of internal Ca^{2+} stores to the transient presynaptic Ca^{2+} signal (in response to a short train of action potentials) was undetectable in en-passant MFBs

(average change in ΔF/F after ryanodine application: + 9 ± 9%, n = 9).
These data provide evidence at the level of single synapses that presynaptic kainate receptors (a) may act as autoreceptors at granule cell – CA3 pyramidal cell synapses, (b) are functionally expressed in a cell-target dependent manner, and (c) involve activation of Ca^{2+} release from presynaptic Ca2+ stores. Whether this functional diversity can explain distinct features of transmission at the respective synapses is currently under investigation.

Supported by Wellcome Trust, Medical Research Council and European Union.

Where applicable, the authors confirm that the experiments described here conform with the Physiological Society ethical requirements.

PC169

Synaptic network of the intercalated neurons in amygdala

R. Geracitano[1], W. Kaufmann[2], G. Szabo[3], F. Ferraguti[2] and M. Capogna[1]

[1]Anatomical Neuropharmacology Unit, MRC, Oxford, UK, [2]Department of Pharmacology, Innsbruck Medical University, Innsbruck, Austria and [3]Laboratory of Molecular Biology and Genetics, Institute of Experimental Medicine, Budapest, Hungary

Intercalated (ITC) cell masses are putative GABAergic neurons located at both borders of the lateral and basolateral amygdala (1). By virtue of its location the intercalated system is ideally situated to gate incoming and outcoming information of the amygdala. ITC neurons are also innervated by cortical fibers and can thus mediate cortical control in a feedforward manner over the basolateral complex and the central nucleus. It has been suggested that ITC cells disinhibit brain stem neurons during fear conditioning by means of their projections to the central nucleus (2). However, information on synaptic connections between ITC neurons is lacking (see also: 3).
Therefore, we are studying properties of unitary GABAergic synaptic responses of ITC cells by using GAD65-GFP transgenic mice. In these mice ITC cells can be identified as clusters of densely packed fluorescent units.
Whole cell patch-clamp recordings were performed with K-gluconate and biocytin containing pipettes in acute coronal slices (330 μm thick, age range: 15-24 days old, recording temperature range: 34-35°C) from ITC neurons mainly located in the intermediate capsula, where fibre bundles between the basolateral complex and the central nucleus are located.
Neurons had heterogeneous passive and active electrophysiological properties (n=83) and were confirmed as ITC after histological processing. Several ITC cells have been reconstructed with the help of a drawing tube and we are currently attempting to correlate their anatomical features with functional properties. Double patch recordings revealed $GABA_A$ receptor-mediated unitary inhibitory postsynaptic currents (uIPSCs) with peak amplitude (mean±SEM) 20.8±3.9pA, rise time 1.4±0.1ms, decay time 12.7±1ms and jitter 0.46±0.05ms (n=28). We found that ITC cells interconnected by at least three modalities, which were identified by fitting with a regression curve (ANOVA, $p<0.05$) the number of uIPSC events plotted against the frequency of stimulation. The three groups were characterised by: 1) synapses that mostly failed at low frequency (0.1Hz) but became responsive at higher frequency of stimulation (10Hz) (n=7); 2) synapses that were activated at 0.1Hz and became unreliable at 10Hz stimulation (n=8) and 3) synapses in which the occurrence of uIPSCs was frequency-independent (n=13). These phenotypes appeared to be linked to differences in release probabilities according to experiments where paired-pulse uIPSCs and manipulation of extracellular calcium concentrations were performed (n=7 and 3, respectively).
Thus, we demonstrate that ITC cell masses are tuned to respond to a wide dynamic range of frequencies and these properties are likely to affect the computational operations of amygdala.

Millhouse OE (1986). *J Comp Neurol* **247**, 246-271.

Pare D *et al.* (2004). *J Neurophysiol* **92**, 1-9.

Marowsky A *et al.* (2005). *Neuron* **48**, 1025-1037.

Funded by MRC UK and IBRO (GR).

Where applicable, the authors confirm that the experiments described here conform with the Physiological Society ethical requirements.

PC170

Mechanism of mitochondrial depolarisation in glutamate excitotoxicity

A.Y. Abramov and M.R. Duchen

Physiology, UCL, London, UK

Pathological activation of glutamate receptors with consequent disturbances in Ca^{2+} homeostasis and collapse of mitochondrial potential plays a major role in the neuronal death that follows episodes of anoxia or ischaemia. We have been concerned to understand the relationships between changes in mitochondrial membrane potential ($\Delta\psi m$) and the failure of cytoplasmic calcium homeostasis following exposure of rat hippocampal neurons to toxic concentrations of glutamate. We have used fluorescence imaging to measure $\Delta\psi m$ and $[Ca^{2+}]_c$ using Rhodamine123 and Fura-FF respectively in primary cultures of hippocampal neurons (10-15 days in vivo). Application of glutamate (100μM) caused a stereotypical response consisting of a delayed loss of $\Delta\psi m$ coincident with a secondary increase in $[Ca^{2+}]_c$. For a period of about 10 min, these responses were reversed by removal of external Ca^{2+}, but after this period, removal of external Ca^{2+} had no effect on either variable. The mitochondrial depolarization but not the secondary increase in $[Ca^{2+}]_c$ was blocked by Ru360 (20 μM), an inhibitor of mitochondrial Ca^{2+} uptake. After prolonged glutamate exposure (10-15 min), when the $[Ca^{2+}]_c$ response had progressed to an irreversible phase and mitochondrial depolarization was complete in most cells, reduction of $[Ca^{2+}]_c$ using the membrane permeant calcium chelator EGTA-AM (50 μM) promoted recovery of $\Delta\psi m$ in the majority of cells (n=169/208 for EGTA-AM), suggesting that the mitochondrial response was dependent on the sustained presence of calcium and was still reversible. Mitochondrial potential also recovered in response to TMPD and ascorbate, which provide electrons to mitochondrial complex IV, suggesting that the effect of calcium involves impaired substrate supply or respiratory chain activity. The mitochondrial substrates methyl-succinate (10 mM) and TMPD (200μM) plus

ascorbate (5mM) recovered potential in the majority neurons (88%, n=79/90 for TMPD/ascorbate; 73%, n=92/126 for Me-succinate) in this period after glutamate addition. In thapsigargin-treated neurons 5μM ionomycin in a Ca^{2+}-free saline raised $[Ca^{2+}]_c$, almost certainly releasing mitochondrial calcium. Furthermore, permeabilisation of the cells with digitonin (10 μM) after 10-15 min glutamate exposure also showed that mitochondria were still intact and were still responsive to additions of calcium and substrates. Thus, after 10-15 min of glutamate exposure mitochondria in hippocampal neurons are still intact, maintain a high calcium content and are able to recover a potential. The loss of potential has been attributed to opening of the permeability transition pore (mPTP) which would lead to loss of mitochondrial calcium and a depolarization that could not be reversed by substrate. We conclude that the early profound mitochondrial depolarization in neurons during excitotoxic glutamate exposure cannot be due to mPTP opening.

Where applicable, the authors confirm that the experiments described here conform with the Physiological Society ethical requirements.

PC171

Diffusion of glutamate in the synaptic cleft

K. Zheng, L.P. Savtchenko and D.A. Rusakov

UCL Institute of Neurology, London, UK

Information processing in the brain is fundamentally constrained by the kinetics of rapid synaptic responses. In turn, the time course of excitatory postsynaptic currents has been shown to depend critically on neurotransmitter diffusion in the synaptic cleft. Most central synapses, however, are not accessible for direct measurements of neurotransmitter concentration because of their small size.

To address this issue, we have focused on common excitatory glutamatergic synapses in the hippocampus (area CA1 in stratum radiatum) and combined two-photon microscopy, patch-clamp electrophysiology and biophysical modelling to assess the speed of glutamate diffusion in the synaptic cleft.

First, we measured the effective diffusion coefficient of small, cell-impermeable soluble 'probe' molecules, the fluorescence indicator Alexa Fluor 350, in area CA1 of acute rat hippocampal slices using rapid two-photon excitation imaging of a diffusion point-source. We have found that perfusing the slices with a 5% solution of 40kDa dextran at 35°C reduces extracellular diffusivity of the probe by 25 ± 3% (n = 30). This reduction was indistinguishable from that in a free medium [1] indicating that interactions with the extracellular milieu play little role in the diffusion-retardation effect of large dextran macromolecules on small, rapidly diffusing molecules. This suggested that dextran should slow down extracellular diffusion of glutamate molecules to a similar degree. Second, we found that dextran application increased the amplitude of evoked (by 16 ± 8%; n = 21), miniature (by 13 ± 7%; n = 6) and minimum stimulation (by 14 ± 4%; n = 8) AMPA receptor-mediated EPSCs recorded in CA1 pyramidal cells (the average increase, 15 ± 4%). Third, we carried out in-depth simulations of glutamate release, diffusion and receptor activation in the typical environment of these synapses using two complementary modelling approaches, multi-compartmental and Monte-Carlo. Taken together, simulation results have proposed a robust non-linear relationship between the amplitude of AMPA receptor mediated responses and glutamate diffusivity in the cleft, as suggested earlier [2-4]. According to this relationship, a 15% reduction of the response amplitude by 25% retardation of diffusion corresponds to a unique value of the glutamate diffusion coefficient inside the cleft (currently estimated in the region of 0.3 μm^2/ms). Subject to the ongoing tests, this value provides a fundamental constrain on interpreting rapid molecular events in the synaptic cleft.

Savtchenko LP & Rusakov DA (2005). Neuroimage 25, 101-111.

Rusakov DA & Kullmann DM (1998). J Neurosci 18, 3158-3170.

Min MY, Rusakov DA & Kullmann DM (1998). Neuron 21, 561-570.

Nielsen TA, DiGregorio DA & Silver RA (2004). Neuron 42, 757-771.

Supported by Medical Research Council and Wellcome Trust.

Where applicable, the authors confirm that the experiments described here conform with the Physiological Society ethical requirements.

PC172

Adenosine A_1 receptors antagonists boost hippocampal gamma oscillations

N. Patel and M. Vreugdenhil

Neurophysiology, University of Birmingham, Birmingham, West Midlands, UK

Caffeine increases cortical activation and the rate and selectivity of information processing (Fredholm et al. 1999), in humans especially in the elderly (Ryan *et al.* 2002). Caffeine exerts these actions most probably through antagonism of the adenosine A_1 and A_{2A} receptors (Fredholm *et al.* 1999), activated by ambient adenosine levels, which are increased with ageing. Hippocampal gamma oscillations are associated with memory (Herrmann *et al.* 2004) and are reduced with ageing (Vreugdenhil & Toescu, 2005). Here we assess the effect of caffeine and selective adenosine receptor antagonists on spontaneous and kainate-evoked gamma oscillations.

Slices (400 μm thick) of the mouse ventral hippocampus were kept at 32°C under interface conditions. Recording electrodes were placed in stratum radiatum of CA3c; intracellular recordings were made from pyramidal neurons in CA3c. In some slices spontaneous gamma oscillations were recorded, otherwise gamma oscillations were induced by addition of 50 nM kainate. Deviation from normal development of power in the gamma range was taken as effect. Caffeine (50 μM) boosted kainate-induced gamma to 225±29% of control levels (n=9, $P<0.01$), without affecting the dominant frequency. Similarly, 50 μM caffeine boosted spontaneous gamma oscillations to 332±111% of control levels (n=9, $P<0.05$), whereas higher concentrations slightly reduced the effect. In some slices without noticeable activity caffeine induced gamma oscillations. The selective A_1 receptor antagonist 8-CPT (5 μM) boosted spontaneous gamma oscillations by 341±22% (n=6, $P<0.01$) times control levels,. Addition of 50 μM caffeine on top of 8-CPT-boosted spontaneous gamma caused a small reduction in gamma power, which

could be mimicked by the selective A_{2A} receptor antagonist ZM241385 (50 nM). However ZM241385 alone had no significant effect.
8-CPT-boosted spontaneous gamma oscillations were resistant to the muscarinic receptor antagonist atropine (5 μM), discarding an A_1 receptor antagonist-induced increase in acetylcholine release (n=6). Intracellular recordings (n=3) showed that 8-CPT caused a 3-5 mV depolarisation, which was associated with a 5-10% increase in input resistance, suggesting the closure of a potassium conductance (O'Kane & Stone, 2004). However, the slow after-hyperpolarisation was not affected by 8-CPT.
These observations indicate that selective A_1 receptor antagonists can induce and/or boost spontaneous gamma oscillations in CA3, by mediating a tonic postsynaptic depolarisation and are therefore potential candidates for cognition-enhancing treatment, especially in the elderly.

Fredholm BB, Battig K, Holmen J, Nehlig A & Zvartau EE (1999). *Pharmacol Rev* **51**, 83-133.

Herrmann CS, Munk MH & Engel AK (2004). *Trends Cogn Sci* **8**, 347-355.

O'Kane EM & Stone TW (2004). *Neurosignals* **13**, 318-324.

Ryan L, Hatfield C & Hofstetter M (2002). *Psychol Sci* **13**, 68-71.

Vreugdenhil M & Toescu EC (2005). *Neuroscience* **132**, 1151-1157.

We thank the MRC for funding this work. We thanks J.G.R. Jefferys for providing a stimulating environment and for the use of equipment.

Where applicable, the authors confirm that the experiments described here conform with the Physiological Society ethical requirements.

PC173

Gap junctions in the adult rat spinal cord: immunohistochemical detection of connexin36 in sympathetic preganglionic neurones

N. Marina[1], D.L. Becker[2] and M.P. Gilbey[1]

[1]Physiology, University College London, London, UK and [2]Anatomy and Developmental Biology, University College London, London, UK

Gap junctional communication in the adult central nervous system plays an important role in the generation of network interactions between areas requiring synchronization of oscillatory activities. In vitro studies have shown evidence of electrotonic coupling through gap junctions between sympathetic preganglionic neurones (spns) in the neonatal and adult rat spinal cord (Logan et al. 1996; Leslie et al. 2000). Electrotonic transmission of membrane oscillations might be an important mechanism for recruitment of neurones and result in the generation of rhythmic sympathetic activity at the population level (Marina et al. 2006).
Gap junctions in the adult spinal cord are constituted principally by connexin36 (Cx36) (Rash et al. 2000). However, the distribution of Cx36 in specific neuronal populations of the spinal cord is largely unknown. In this study we aim to identify the presence of Cx36 in spns along the thoraco-lumbar spinal cord of the adult rat. Adult Sprague Dawley male rats (280-300gr, n=6) were deeply anaesthetized with urethane (1.3g/kg, IP) and intracardially perfused with paraformaldehyde. The spinal cords and brainstems were collected, postfixed for 60 min and cryo-protected. Double immunostaining against Cx36 (Bittman et al. 2002) and choline acetyltransferase (ChAT) was performed on horizontal sections (20 μm) taken from spinal segments T1-T3, T6-T8, T10-T11, L1-L2. Positive and negative controls were performed in sections of caudal medulla (inferior olive) and spinal cord (motoneurones) to assay specificity of staining for Cx36 and ChAT, respectively. In all the spinal cords analysed, Cx36 punctate immunostaining was greatest in lower thoracic and lumbar segments and it was distributed in the grey and white matter. Cx36 punctate staining was consistently detected in ChAT-immunoreactive neurones from the intermediolateral cell column (IML) and the central autonomic nucleus (CAN). Cx36 puncta were distributed mainly along dendritic processes and to a lesser extent, in neuronal somata. The presence of Cx36 in spns is consistent with electrical coupling between spns through gap junctions in the adult spinal cord.

Bittman K *et al.* (2002). *J Comp Neurol* **443**, 201-212.

Leslie J *et al.* (2000). *J Physiol* **582P**, 108P.

Logan SD *et al.* (1996). *J Physiol* **495**, 491-502.

Marina N *et al.* (2006). *J Physiol* **571**, 441-450.

Rash JE *et al.* (2000). *Proc Natl Acad Sci* **97**, 7573-7578.

This work was supported by the Wellcome Trust (grant number 063954).

Where applicable, the authors confirm that the experiments described here conform with the Physiological Society ethical requirements.

PC174

Structured spike trains alter excitability

R. Dyball and J. Hawton

University of Cambridge, Cambridge, UK

Spikes recorded from single cells do not occur regularly. Interspike intervals show great variation. Since all spikes have the same amplitude, the intervals between them must carry any information they code for. Recently developed measures of spike activity have been shown to change in response to physiological stimuli. Cells in the suprachiasmatic nucleus show different activity at different times of day (Bhumbra et al. 2005a) and ADH cells alter their activity after osmotic stimulation (Bhumbra et al. 2005b). We investigated whether different interval patterns that potentially carried coded information altered the threshold for antidromic activation of the cells we recorded. Using the standard ventral approach to the hypothalamus and conventional recording techniques, we recorded extracellularly from neurohypophysial cells in urethane-anaesthetised (1.2 g/kg

IP) rats and applied stimulus pulses to their axons. We found that trains of as few as 3 pulses with a 20 ms interval profoundly affected the threshold for stimulation. Short bursts of pulses lowered threshold, probably by depolarising the axon at the stimulus site. The decreased threshold was seen if stimulus interval was increased to 40 or 80 ms but was not seen if the interval between the stimuli was increased to 100 ms. The effect was seen in all 19 cells tested. In a representative experiment with trains of 5 stimuli, the 5th pulse evoked an antidromic spike 10/10 times with a 20 ms interval, 5/10 times with an 80 ms interval but never (0/10 times) with a 100ms interval. This suggests that, whatever the mechanism, the effect lasted only for 100 ms. By contrast, longer trains of pulses (10–20 pulses with a 20 ms interval delivered each second) raised threshold (in 15 of 20 cells tested). Under the conditions of the experiments, the effect lasted up to 30 s. The raised threshold occurred even if the interval between stimulus pulses was increased to 80 ms. Intracellular recordings (from the cell bodies of neurohypophysial cells) showed that brief bursts of (~10) spikes induced by intracellular injection of depolarising current lowered resting membrane potential (by 2-3 mV, probably by activating calcium gated potassium channels). It thus appears that the intervals between spikes profoundly affected the excitability of the axons of the recorded cells. The variability and patterning of spike interval distribution may thus carry information particularly if the changes in membrane potential alter the propagation of spikes across branch points in the region of axon terminals.

Bhumbra GS, Inyushkin AN, Saeb-Parsy K, Hon A & Dyball REJ (2005a). J Physiol 563, 292–307.

Bhumbra GS, Inyushkin, Syrimi M, & Dyball REJ (2005b). J Physiol 569, 257-274.

Where applicable, the authors confirm that the experiments described here conform with the Physiological Society ethical requirements.

PC175

The mitochondrial K_{ATP} channel opener BMS-191095 reduces neuronal damage after transient focal cerebral ischaemia in rats

D. Busija, B. Kis, K. Mayanagi and T. Gáspár

Physiology/Pharmacology, Wake Forest University Health Sciences, Winston-Salem, NC, USA

Activation of mitochondrial ATP-sensitive potassium channels (mitoKATP channels) appears to protect the brain against ischaemic or chemical challenge (1). Unfortunately, the prototype mitoK_{ATP} channel opener, diazoxide, has potassium channel-independent pathways (2). We examined potential effects of BMS-191095, a novel, selective mitoK_{ATP} channel opener, against transient middle cerebral artery occlusion (MCAO) in rats (3). Experiments were performed on male Wistar rats subjected to 90 min of MCAO. Anesthesia was induced with 5% halothane in a 70:30 gas mixture of N_2O and O_2. Endotracheal intubation was performed, and all the animals were mechanically ventilated with 1.0-1.5% halothane in a 70:30 gas mixture of N_2O and O_2. BMS-191095 (25 μg; estimated final brain level of 40 μM, n=12) or vehicle was infused into the left lateral ventricle prior to the onset of ischaemia. We also examined effects of BMS-191095 on mitochondrial membrane potential and reactive oxygen species (ROS) production in cultured cortical neurons isolated from rat E18 fetuses. Mitochondrial membrane potential was monitored using the specific detection dye tetramethylrhodamine ethyl ester (TMRE, Molecular Probes). Treatment with BMS-191095 24 hr before the onset of ischaemia reduced total infarct volume by 29% (206.2 ± 16.5 to 149.2 ± 18.2 mm^3; $p<0.05$) and cortical infarct volume by 34% reduction (144.2 ± 15.4 to 95.2 ± 14.4 mm^3; $p<0.05$). However, treatment with BMS-191095 given 30 or 60 min prior to MCAO did not reduce infarct volume ($p<0.05$). Protective effects of BMS-191095 were completely prevented by co-treatment with 5-hydroxydecanoate (5-HD), a mitoK_{ATP} channel antagonist. In neurons, BMS-191095 (40 μM) depolarized the mitochondria without affecting levels of ROS, and this effect was inhibited by preincubation with 5-HD. In conclusion, BMS-191095 effectively protected the brain against MCAO in the rat, suggesting that selective opening of mitoK_{ATP} channels with BMS-191095 induces delayed preconditioning against transient focal ischaemia without non-specific effects such as generation of ROS.

Busija DW, Lacza Z, Rajapakse N, Shimizu K, Kis B, Bari F, Domoki F & Horiguchi T (2004). Brain Res Rev 46, 282-294.

Nagy K, Kis B, Rajapakse NC, Bari F & Busija DW (2004). J Neurosci Res 76, 697-704.

Kis B, Nagy K, Snipes JA, Rajapakse NC, Horiguchi T, Grover GJ & Busija DW (2004). Neuroreport 15, 345-349.

Supported by grants HL30260, HL66074, and HL77731 from the National Institutes of Health, and AHA Bugher Foundation Award 0270114N from the American Health Association.

Where applicable, the authors confirm that the experiments described here conform with the Physiological Society ethical requirements.